LRP 305/86 August 1989

EFFICIENCY OPTIMIZATION FOR QUASI-OPTICAL GYROTRONS

B. Isaak, A. Bondeson, M.Q. Tran, A. Perrenoud,
S. Alberti and P. Muggli

EFFICIENCY OPTIMIZATION FOR QUASI-OPTICAL GYROTRONS

B. Isaak, A. Bondeson, M.Q. Tran, A. Perrenoud,
S. Alberti and P. Muggli

Centre de Recherches en Physique des Plamas
Association Euratom - Confédération Suisse
Ecole Polytechnique Fédérale de Lausanne
21, Av. des Bains, CH-1007 Lausanne /Switzerland

ABSTRACT

Optimization studies for resonator cavities of quasi-optical gyrotrons have been carried out. With the constraint that the RF field is limited by peak power load on the mirrors, the electronic efficiency can have a value of up to 10% higher than the confocal results by using spherical mirrors with g=1-d/R close to -1. Optimized nonspherical cavities yield similar results. When output coupling through circular slots is considered, confocal (g=0) as well as more extreme designs near the resonator stability boundary are less favorable and the optimum configurations found are spherical mirrors with g-factors of about -0.3, -0.6, and possibly -0.75.

1 INTRODUCTION

It is well known that in conventional gyrotrons the efficiency is strongly dependent on the shaping of the RF field profiles along the direction of beam propagation. As part of the quasi-optical gyrotron project at the CRPP Lausanne, we have carried out extensive efficiency optimization studies for various resonator designs. A main objective was to find out whether, for example, cavities with nonspherical mirrors might lead to significant improvement of efficiency.

Quite generally the efficiency of interaction increases with increasing RF field strength up to a certain field value from when on the effect of overbunching of the beam decreases again the efficiency However, an important consideration in the design of a steady state system is that the heat load on the mirrors is limited [2]. We have therefore carried out the optimization keeping the maximum local power dissipation fixed. Furthermore, since with a quasi-optical resonator, power can be lost outside the output coupling structure [2], we have considered the total efficiency, i.e. the product of electronic and output coupling efficiency. In all cases quoted, results refer to the maximum single mode efficiency after optimization with respect to frequency detuning and tapering of the background field $B_0(z)$.The results of the optimization study have been presented at the 11th International Conference on Infrared and Millimeter Waves in Pisa [7].

2. GENERAL REMARKS

2.1. Short Description of the General Resonator Configurations

The numerical calculations have been done with a resonator code that calculates the eigenmodes - the complex electric field E - and the eigenvalues for general mirror configurations using the Huygens-Fresnel integral equations. This generalized mirror programme enables one to consider within the paraxial approximation deviations of the mirror surfaces from the standard spherical shape. A schematic description of the resonator configuration is given in (Fig 1). In a second step the calculated electric field distribution in the beam plane is implemented into the gyrotron equations of motion for the electrons.

In terms of the coordinate system described in (Fig 1) we characterize a general nonspherical mirror with a function $\delta y(x,z)$ of the mirror coordinates x and z giving the deviation in the y-direction from an underlying spherical surface; positive values leading to an increased curvature of radius. In the optimization study we have restricted ourselves to the three following resonator configurations:

a) resonators with spherical symmetric mirrors (Fig 2a) characterized by the g-factor ($g=1-d/R$, where R is the radius of curvature of the spherical surface and d is the mirror distance). A detailed description of such mirror systems can be found for example in [6]. In the computations reported here, we have used the spherical approximation for the surface,i.e. its deviation from a plane parallel to the x-z-plane is $\Delta y_S=r^2/(2R)$, where $r^2=x^2+z^2$. The diffraction loses of a resonator with spherical mirrors depend on g and the Fresnel number $N=a^2/\lambda d$, where a is the mirror radius and λ the wavelength of the E-field.

b) resonators with ellipsoidal mirrors (Fig 2b), which are characterized by the two independent radii of curvature R_x and R_z, in the x and z directions, respectively. For small x and z the deviation in the y-direction from the (x,z) plane is $\Delta y=x^2/2R_z + z^2/2R_z$.

We can define in analogy to case a) two corresponding g-factors in the directions x and z :

$$g_x = 1-d/R_x \qquad (2.1.1)$$
$$g_z = 1-d/R_z$$

The deviation from the underlying spherical surface with a radius of curvature R and the corresponding g-factor $g = 1-d/R$ is

$$\delta y(x,z)=\Delta y-\Delta y_S = \frac{g_x-g}{2d}x^2 + \frac{g_z-g}{2d}z^2 \qquad (2.1.2)$$
$$= s_x\frac{x^2}{d} + s_z\frac{z^2}{d}$$

where the coefficients s_x and s_z are defined as

$$s_x=(g_x-g)/2 \qquad (2.1.3)$$
$$s_z=(g_z-g)/2$$

In the calculations we choose either $s_x=0$ or $s_z=0$, e.g. $R_x=R$ or $R_z=R$ (Fig 2b). The deviation δy is then a quadratic function of either x or z only.

c) resonators with non-symmetric mirrors that are spherical on one half and ellipsoidal on the other (Fig. 2c). For such cases, the function δy (deviation from the spherical surface) is a quadratic function of z for either the negative or positive z-values ($\delta y=s_z \cdot z^2$) and equal to zero otherwise ($\delta y=0$). To simplify the subsequent discussion we define separate g-factors in the z-direction on the positive and negative sides as g^+ and g^-.

The electric field profiles of the fundamental modes of the above mentioned resonator types are in case a) rotationally symmetric around the axis y, in b) independently symmetric in the x and z coordinates and in c) symmetric only in x. As illustration for the above cases, Figs 2a), b) and c) show in an axonometric representation the three different mirrors types.

2.2 Basic relations for spherical resonators

In the following chapter a short summary of some basic relations for spherical resonators is given. We refer the reader to [2] for a more detailed study. If the mirror radius is large compared to the spot size w the field of the fundamental mode TEM_{00} of such a resonator is to a good approximation gaussian in the x-z-plane, and has a standing wave pattern in the y-direction. For a linearly polarized field E_x in the x-direction, the E-field is

$$E_x(x,y,z,t) = E(x,y,z) \sin (k_y y + \alpha(x,y,z)) \cos \omega t \qquad (2.2.1)$$

where $k_y=\omega/c$ (ω is the angular frequency and c the speed of light)

$$E(x,y,z) = E_0 \left(\frac{w_0}{w_s(y)}\right) e^{-(x^2+z^2)/w_s^2(y)} \qquad (2.2.2)$$

$$\alpha(x,y,z) = R^{-1}(y) (x^2+z^2) \frac{\omega}{2c} - \tan^{-1} \left(\frac{y}{y_R}\right)$$

$E_0 \left(\frac{w_0}{w_s(y)}\right)$ is the peak amplitude at given y position

with w_0 the minimum spot size at y=0, $w_s(y)=w_0(1+y^2/Y_R^2)$ is the spot size in the plane y=const, $Y_R=w_0^2\,\omega/2c$ is the Rayleigh length, and $R_y=y(1+Y_R^2/y^2)$ is the radius of curvature of the spherical wavefront.

The spot sizes on the mirrors (with, in general, different g-factors) and in the beam plane depend on the g-factors and the parameter $r_0=(d/k)^{1/2}$, where $k = 2\pi/\lambda$ and λ is the wavelength. We have the following relations :

- in the beam plane :

$$w_0^2 = 2r_0^2 \sqrt{g_1g_2(1-g_1g_2)}\ /\ (g_1+g_2 - 2g_1g_2) \qquad (2.2.3)$$

or, if $g_1 = g_2 = g$

$$w_0^2 = r_0^2 \sqrt{\frac{1+g}{1-g}}$$

- on mirror 1 :

$$w_1^2 = 2\, r_0^2 \sqrt{\frac{g_2}{g_1}\frac{1}{1-g_1g_2}} \qquad (2.2.4)$$

or if $g_1 = g_2 = g$

$$w_1^2 = 2\, r_0^2 \sqrt{\frac{1}{1-g^2}}$$

-on mirror 2 :

$$w_2^2 = 2r_0^2 \sqrt{\frac{g_1}{g_2}\frac{1}{1-g_1g_2}} \qquad (2.2.5)$$

A special case is the confocal resonator g=0 with $w_0=r_0$ and $w_1=w_2=(2r_0)^{1/2}$.

Due to the conservation of the power flux the peak amplitudes of the electric field of the travelling wave component in the beam plane E_b and at the mirrors E_m are related.

$$w_m E_m = w_b E_b$$

$$\frac{E_b}{E_m} = \frac{w_m}{w_b} = \sqrt{\frac{2}{1+g}} \qquad (2.2.6)$$

The central value of the electric field for the standing wave in the beam plane is twice the above value.

The ohmic heat losses on the mirrors impose an important technological constraint since the peak thermal loadings on the mirrors should not exceed the maximum values which depend on the material and the cooling technology. The heat losses on each mirror are given by

$$L_i = \int_M \frac{2}{Z_0^2 \sigma \delta} |E_{in}(\vec{r})|^2 \, d^2r \qquad [W] \qquad (2.2.7)$$

where $Z_0 = \sqrt{\mu_0/\varepsilon_0} = 377\ \Omega$, σ the conductivity and $\delta = (\omega\mu_0\sigma/2)^{-1/2}$ the skin depth.

For spherical mirrors and a gaussian beam the heat loss is related to the peak amplitude of the incoming wave.

$$L_i = \frac{\pi w_m^2}{Z_0^2 \sigma \delta} |E_{io}|^2 \qquad [W] \qquad (2.2.8)$$

The relation between the heat power flux and the electric field

$$P_{ohmic} = \frac{2}{Z_0^2 \sigma \delta} |E|^2 \qquad [W/m^2] \qquad (2.2.9)$$

then leads to the following relation

$$L_i = \frac{\pi w_m^2}{2} P_{ohmic,max}, \quad P_{ohmic,max} = \frac{2}{z_0^2 \sigma \delta} |E_o|^2 \qquad (2.2.10)$$

between the total heat loss L_i and the maximal thermal load per unit area (at the center of the mirror) P_{max}. As a reasonable value we shall take the maximal heat load on the mirror to be below 1.5 kW/cm^2. The average heat load P_{ohmic}/(mirror surface) is of course smaller and this would allow for some margin in the selection of the maximal permissible E-field value. In Table I, we give specific values for the corresponding permissible maximal electric fields in the cases of copper and brass mirrors.

2.3 Electron orbit calculation

We refer the reader to [1] for a detailed description of the single-mode nonlinear computations in quasi-optical gyrotrons. To take into account the non-gaussian nature of the cavity field we allow the amplitude $E_0(z)$ and the phase $\delta(z)$ to be specified as arbitrary functions of z.

$$E \approx \mathrm{Re}\,(E_0(z)e^{-(x^2+z^2)/w_0^2}e^{i(\omega t+\delta(z))})$$

This additional dependency of the phase $\delta(z)$ in the direction of the propagating beam could have an influence on the gyrotron interaction efficiency of similar nature as the magnetic field tapering.
The basic equations of motion (using guiding center variables and the slowly varying phase angle θ) are

$$\frac{dp_\perp}{dz} = \frac{-em\gamma}{2p_z} E(z) \sin ky_g \cos\theta \qquad (2.3.1)$$

$$\frac{d\theta}{dz} = \frac{m}{p_z}\left(\Omega - \gamma\omega - \frac{d\delta(z)}{dz}\right) + \frac{m\gamma e\, E(z)}{2p_\perp p_z} \sin ky_g \sin\theta \qquad (2.3.2)$$

$$\frac{dy_g}{dz} = 0 \qquad (2.3.3)$$

$$\Omega = \frac{eB_0}{m} \qquad B_0 \text{ is the external magnetic field}$$

Note the additional term $-d\delta(z)/dz$ in the second equation as compared to the equation in [1]. The slowly varying phase angle θ is now defined as

$$\theta = \Psi - \omega t - \delta(z) \qquad (2.3.5)$$

where Ψ is the gyrophase of the electron. In the numerical calculations we use a pencil beam placed at a maximum of the electric field in the y-direction.

2.4 Comments on ellipsoidal mirrors

Under the assumption that $p_\perp^2 \gg p_z^2$ and $\gamma - 1 \ll 1$ $(\gamma = (1-\beta^2)^{-1/2} \approx 1+p_\perp^2/2m^2c^2)$ and assuming a gaussian field profile one can derive a set of approximate scaling laws [1] for the electron orbit equations.

$$\frac{d\rho}{d\xi} = -\varepsilon_e^{-\xi^2} \cos\theta \sin ky_g \tag{2.4.1}$$

$$\frac{d\theta}{d\xi} = \Delta - \kappa\rho^2 + \left(\frac{\varepsilon}{\rho}\right) e^{-\xi^2} \sin\theta \sin ky_g \tag{2.4.2}$$

with the dimensionless variables and parameters

$$\rho = \frac{p_\perp}{p_{\perp 0}} \quad , \quad \xi = \frac{z}{w_b} \tag{2.4.3}$$

$$\varepsilon = \frac{eEw_b}{2\beta_z\beta_{\perp 0}mc^2} \qquad \Delta = \frac{w_b(\Omega-\omega)}{c\beta_z} \tag{2.4.4}$$

$$\kappa = \frac{\omega w_b \beta_{\perp 0}^2}{c\beta_z}$$

For β_z and $\beta_\perp$ fixed, one sees that two important quantities are $E\cdot w_b$ and $\omega\cdot w_b$. In [3] it was shown that the optimum value for w_b/λ lies around 4.8 with the electronic efficiency changing only slightly in the range of $3.8 < w_b/\lambda < 5.5$. For a gaussian field profile $w_b/\lambda = (d/2\pi\lambda)^{1/2} \cdot (1+g/1-g)^{1/4}$ so that for constant d and λ the g-factors should preferably lie in the range $|g|<0.5$ in order for w_b/λ to be near the optimum value. The dependency on w_b/λ is not very strong as compared to that on the other parameter $E\cdot w_b$ not very strong. To have a high efficiency it is necessary to have a large $E\cdot w_b$ The results mentioned in [3] show that for normalized values $\sqrt{\pi}eE\cdot w_b/mc^2$ greater than 0.2 one obtains high electronic efficiencies. It must be pointed out though that a too large value $r(\pi)eE\cdot w_b/mc^2$ (greater than 0.6) can lead to overbunching of the beam and therefore a loss in efficiency. One can roughly say, taking always the above remark into consideration though,that a long interaction region w_b and/or a high E-field maximum (restricted by the maximal heat load on the mirrors) lead to high electronic efficiencies. For spherical resonators we have due to energy conservation

$$E_b \cdot w_b = \sqrt{2}\, E_m \sqrt[4]{\frac{1}{1-g^2}} \qquad (2.4.5)$$

where E_m is the field on the mirror.

One immediately sees that if the maximum field on the mirror is kept constant, $E_b \cdot w_b$ diverges when $g \rightarrow \pm 1$.

For spherical mirrors E_b and w_b are not independent of each other at a fixed E-field value on the mirrors. However the two variables can be decoupled though if we consider ellipsoidal mirrors. The basic idea is to increase the spot size in the parallel direction (with regard to the B-field) and to decrease the spot size in the transversal direction, thus increasing the interaction region and the E-field maximum at the same time. Recall that for spherical mirrors $E_b w_b = E_m \cdot w_m$, so that $E_b = E_m \cdot (2/(1+g))^{1/2}$ which diverges for $g \rightarrow -1$. Similarly the beam spot size $w_b^2 \sim (1+g/1-g)^{1/2}$ diverges for $g \rightarrow +1$. Let us for the moment consider ellipsoidal resonators with infinite mirror radii so that the Huygens-Fresnel integral equation becomes separable. The E-field is then of the form

$$E = E_0\, e^{-x^2/w_x^2 \,-\, z^2/w_z^2} \qquad (2.4.6)$$

where w_x and w_z are the respective spot sizes in the x and z direction.

The flux $\int |E|^2\, dxdy$ is then given by $E^2 w_x w_z = E^2 \bar{w}^2$ where we have defined an average spotsize $\bar{w} = \sqrt{w_x \cdot w_z}$. The conservation of flux leads to the relation

$$E_b = E_m \cdot \frac{\bar{w}_m}{\bar{w}_b} = E_m \sqrt{\frac{w_{mz} w_{mx}}{w_{bz} w_{bx}}} \qquad (2.4.7)$$

The interesting quantity, interaction length x E-field, becomes

$$E_b \cdot w_{bz} = E_m \sqrt{\frac{w_{mx}}{w_{bx}}}\, w_{mz} w_{bx} \qquad (2.4.8)$$

$$= \sqrt{2}\, r_0\, E_m \sqrt{\frac{1}{(1+g_x)(1-g_z)}}$$

One immediately sees that in order to achieve high efficiency it is advantageous to have large negative g_x and large positive g_z.

2.5 Asymmetric mirrors

The reason for using asymmetric mirrors lies in the possibility of deforming the field profile in the beam plane so as to optimize the energy extraction from the electron beam as is done in conventional gyrotrons [8]. Qualitatively one expects that to yield high efficiency the profile must at first increase slowly in amplitude,enabling the electrons to bunch properly, then abruptly decrease after the E-field peak value to prevent the electrons from regaining energy from the field. By using non-spherical mirrors one can deform the gaussian field profile in the desired manner. In addition the resulting variation of the field phase $\delta(z)$ may be used or a replacement for tapering of the B-field.

Numerically the complex electric field (absolute value E(z) and phase $\delta(z)$) are calculated first in the general resonator code to be subsequently used in the single-mode code with specified beam characteristics. In our study we have used a beam with a pitch angle = 1.0 (α= 1.56) and an energy γ =1.137

3. DESCRIPTION OF RESULTS

As mentioned previously we restrict ourselves to spherical, ellipsoidal and asymmetric mirror configurations. The maximum value for the electric field on the mirrors is kept fixed to correspond to a given maximum heat load. We have considered at first resonators with 4% total diffraction losses. By varying the mirror shape and keeping the maximum field value on the mirrors fixed one varies not only the profile but also the value of the electric field maximum in the beam plane, so that one cannot clearly distinguish the various effects (E-field maximum, field profile, spot size) on the electronic efficiency from each other. In a first step we investigate the influence of various mirror configurations on the electronic efficiency without considering the problem of output coupling. In a second step mirrors with output coupling slots are considered. The total efficiency, defined as the product of the electronic and output coupling efficiencies, is then optimized. The present study is not fully self-consistent in the sense that we have computed the maximum single-mode efficiency after optimization with respect to frequency detunning. The question of mode competition and accessibility of the spectrum mode is not addressed

here. In addition all efficiencies are quoted as optimized with respect to the tapering of the background field $B_0(z)$. In the following figures we therefore plot the electronic efficiency as function of the frequency detuning Ω/ω and the magnetic field tapering $\Delta B/B$.

3.1 Stability region

It is well known that for spherical mirrors the resonator becomes unstable if $g \rightarrow \pm 1$ [6]. In geometrical optics terminology the field in stable resonators is bounded by caustic surfaces [5], whereas for unstable resonators no such surfaces exist. We have investigated the stability of ellipsoidal and asymmetric resonators by calculating the diffraction losses of the various resonators keeping the inner radii fixed. In the ellipsoidal case we find that indeed for $-1 < g_x < 1$ and $-1 < g_z < 1$ the resonator is stable (region of low losses) (Fig. 3). Resonators with asymmetric mirrors show a somewhat more complicated stability behaviour. In general asymmetric increases the diffraction losses (Fig. 4). When the deviation from the underlying spherical surface, given by the parameter s defined such that $g_z = g+2s$ is small one has the familiar stability condition $|g|<1$. In general, one can say that the resonator has high losses if the averaged g_z-factor $\bar{g}_z=(1/2)(g_z^+ + g_z^-)$ approaches ± 1. It is interesting to note that there are regions where the modes with the lowest losses are no more the fundamental (q,0,0) modes. In such anomalous regions the diffraction losses tend to be high. (One such area, visible in (Fig. 4) runs diagonally across the contour plot in the upper right hand corner region). In such regions, the properties of the resonator are very sensitive functions of the parameters, and it appears that they are not of interest for practical use.

3.2 E-field in beam plane

As mentioned previously it is desirable to have a high maximum E-field in the beam plane. For spherical mirrors the E-field increases with decreasing g. For asymmetric and ellipsoidal mirrors we expect a similar result. In Fig. 5, we plot the E-field maximum for asymmetric mirrors. The maximum value is reached when $g \rightarrow -1$. At a fixed value for the g-factor of the underlying spherical surface one increases the E-field by decreasing the radius of curvature R_z. The deviation $\delta y = s_z \cdot z^2$ will then become more and more negative. There is, however, a saturation value for δy at which the E-field is at a maximum. For ellipsoidal mirrors (Fig. 6) one has a similar result so that at a fixed g-factor in one direction one can increase the E-field by decreasing the

curvature in the other direction. In conclusion one can say that a high E-field is achieved near the boundary g→-1; the inclusion of ellipticity or asymmetry increases the value slightly.

3.3 Electronic efficiency

The electronic efficiency, defined as the normalized difference between the beam energy entering and leaving the cavity ($\eta=(\gamma_0-\langle\gamma\rangle)/(\gamma_0-1)$) will depend on the mirror shape since the various mirror configurations have different complex E-field profiles. In the following we take the results for the spherical mirrors as a reference point and compare the electronic efficiency for ellipsoidal and asymmetric mirrors therewith. In the numerical calculations the electron beam parameters are kept fixed at the values $\gamma_0=1.137$ and $\beta_\perp/\beta_\parallel=1.56$. The E-field is fixed to give a maximal heat load of 1.1kW/cm^2 on the mirror.

a) Spherical mirrors

In the case of spherical mirrors one can achieve very high E-field maxima in the beam plane by going to large negative g-factors but only at the cost of decreasing the interaction length (Fig. 7). The numerical calculations show that one indeed achieves a high electronic efficiency near g=-1 due to the increase in the E-field. As seen from Fig. 8, the scan over the g-factors from -.9 to +.9 shows a maximal efficiency value $\eta=53\%$ at g=-.9. The efficiency then drops rapidly to 40% near the confocal case g=0.

The following constraints must be taken into consideration :

1) The resonator should be stable, e.g. should not be to close to g=-1.

2) At large negative values for g the losses between TEM_{ooq} and TEM_{10q} modes become comparable [7].

3) If one considers an annular beam with a radius r_b then the variation of the field profile in the x-direction can become important. The optimum value for the beam radius for instance in the case of a 200kW gyrotron with a current of 10A is given by $kr_b\approx5$ [1] e.g. $r_b/\lambda\approx5/2\pi$. Comparing with the desired optimum for the spot size as given by $w_0/\lambda\approx5$ one sees that

$r_b \approx 1/6\ w_0$ so that the spatial variation of the gaussian field profile in the x-direction is negligible. In the case of a 1MW gyrotron the realistic value of r_b due to space charge is assumed such that $kr_b \sim 10\text{-}20$ so that r_b and w_0 become comparable and the variation of the E-field in the x-direction will decrease the efficiency. By going to lower negative g-factors the spot size becomes smaller so that the efficiency is furthermore decreased. The restriction that for annular beams $r_b < w_0$ therefore imposes a lower limit on the g-values.

Taking the above comments into consideration makes it reasonable to restrict the g-factors to values above g=-.7, where the electronic efficiency is about 44%.

b) Ellipsoidal resonators

As previously mentioned the possibility of using ellipsoidal mirrors lies in the possibility of increasing the interaction region and at the same time increasing the E-field in the beam plane by going to large negative g_x and large positive g_z. A scan over the values for g_x=-.8 to -.1 and g_z=-g_x yields indeed a maximum electronic efficiency of 48% at g_x=-.8. The efficiencies are slightly higher as compared to the corresponding spherical mirrors ($g=g_x$). For instance the ellipsoidal case with g_x=-.7 and g_z=+.7 yields 45% as compared to 44% for the spherical case. Numerous other ellipsoidal configurations have been calculated giving however efficiencies less than the above value of 48%. In the case of an annular beam one must take a similar constraint on g_x into consideration as mentioned in the previous paragraph, namely that the resulting spot size in the x-direction should be sufficiently larger than the beam radius.

c) Asymmetric mirrors

The calculations show that asymmetric mirrors can increase the electronic efficiency. However too large an asymmetry leads to unstable resonators. A good efficiency of around 55% can be achieved by using nearly spherical mirrors with a large negative underlying g-factor and a slightly negative surface deviation δy, thus decreasing the curvature R_z on the lower mirror half. As an illustration Fig. 10 represents a scan over some asymmetric mirror configurations (corresponding to a diagonal cut in Fig. 4 such that the averaged g_z-factor $\bar{g}_z = 1/2(g_z^+ + g_z^-)$ is near -1). The efficiencies lie between 50%

and 55%. Figure 11 shows asymmetric configurations with a fixed underlying g-factor $g=g_x=g_z^+=-.6$ and decreasing g_z^-. As to be expected the efficiency increase with decreasing g_z^-. Here again we must take the same constraints as mentioned in the previous section on spherical mirrors into consideration. As an example for a realistic value of $g=-.6$ and $g_z^-=-.8$ one achieves an efficiency of 42%.

3.4 Efficiency optimization under the restriction of output coupling through slots

The previous calculations show that one can reach a high efficiency using large negative g-factors. As mentioned in [3], one important disadvantage of large g-factors is that one has poor output coupling through slots. If one includes such slots the important quantity to be optimized will then be the total efficiency defined as the product of the electronic and output coupling efficiencies. The output coupling efficiency c_{eff} is defined by

c_{eff} = power flux through slots/total diffracted power flux.

We have restricted the calculations to resonators with a fixed diffraction loss of 4% and an output coupling through circular slots. The outer mirror radius is kept fixed at 70mm and the outer slot radius at 43.5mm. The inner mirror slot radius is then adjusted for each resonator configuration to yield the 4% diffraction losses. Furthermore, we have kept the distance between the mirrors fixed at 360mm. The above values have been chosen to match with the present experimental setup at the CRPP.

The numerical calculations for various mirror configurations (spherical, ellipsoidal and asymmetric) show that a maximum value of 90% output coupling efficiency is achieved for spherical mirrors with a g-factor of $g=-.3$. Another maxima with an efficiency of 87.5% is located at $g=-.75$. In general under the restrictions described earlier the use of ellipsoidal or asymmetric mirrors decreases the output coupling efficiency.

We have additionally studied two resonators with spherical mirrors that have much higher diffraction losses (e.g. 10% and 20% losses). The result is that the output coupling efficiency attains high (around 90%) and more stable values with respect to varying g-factors over a slightly larger range (see also comments in 3.5 and Figures 16a and b).

The optimum for the total efficiency has been sought for in the vicinity of these two local maxima of the output coupling efficiency by slightly varying the ellipticity and asymmetry of the mirrors.

The optimization results are summarized in the following sections.

a) Ellipsoidal mirrors

The optimum values for the total efficiency are seen to be near the spherical configurations. Around the value of g=-.3 one has a total efficiency of 35% with an electronic efficiency of 41%. Near g=-.75, the total efficiency of 42% is higher due to the increase in the electronic efficiency (48%). Figure 14a) shows the results for the spherical mirrors and Figures 14b) and c) illustrate the dependency of the efficiencies on the ellipticity at a fixed g-factor in the x-direction g_x=-.3 and g_x=-.75 and varying g_z.

b) Asymmetric mirrors

For asymmetric mirrors the departure from the spherical configuration decreases the output coupling efficiency but increases the electronic efficiency. Around g_x=-.3 one finds optimum values at g_z^-=-.1 and g_z^-=-.4 where the total efficiency becomes slightly higher than the value for the spherical configuration. In the first case where g_z^-=-.1 the interaction region for the electron beam is slightly increased, thus increasing the electronic efficiency whereas in the second case the E-field is increased. The other optimum is achieved at g=-.75 near the spherical configurations at g=-.75. Figures 14d), e), f) and g) illustrate the influence of asymmetric mirrors on the overall efficiencies.

3.5 Additional results for spherical resonators

Increasing the maximal permissible heat load increases the E-field in the beam plane. Figures 15a) and b) show the efficiency plots for such different E-field values. We note that at the higher values of the E-field the electronic efficiency can become smaller at large negative g-factors because the electron beam becomes overbunched due to the increased E-field value.

It is reasonable to expect that for resonators with higher diffraction losses the output coupling problem becomes less pronounced. Figures 16a) and b)

illustrate the behaviour of the output coupling and electronic efficiency for resonators with such high diffraction losses (10% and 20%). In general one sees that the output coupling reaches efficiencies around 90% over a wider range in the g-factor as compared to resonators with 4% losses. (In the calculations the mirror radius is fixed at 70mm and the outer slot radius at 43.5mm.)

By increasing the mirror radius one forces the microwave power through the slots, thus increasing the output coupling. We have made a scan of the output coupling efficiency at various values for the mirror radius and outer slot radius. Increasing the mirror radius indeed gives somewhat better output coupling efficiencies of up to 93%.

CONCLUSIONS

Resonators with large negative g-factors and non-spherical mirrors yield good electronic efficiency. The lower limit for the g-factor depends on the constraints mentioned in 3.1. With realistic values for the g-factor in the range $-.7<g<-.5$ yield one can obtain electronic efficiencies between 43% and 45% as compared to the confocal result of 40%.

The overall picture gained from the output coupling calculations show that the problem of output coupling is of crucial importance if one wishes to go to larger negative g-factors ($g\leq-.5$) or use ellipsoidal or asymmetric mirrors. Using circular output coupling slots and the previously specified resonator parameters a good value for the total efficiency ($\eta_{total}=42\%$) is achieved near the spherical symmetric configuration with an underlying g-factor of -.75. For such resonators the balance between output coupling efficiency and electronic efficiency is at an optimum. By increasing the ellipticity or asymmetry of the mirrors one can increase the electronic efficiency but at the cost of the output coupling efficiency.

ACKNOWLEDGEMENT

This work was partly supported by the "Commission pour l'Encouragement de la Recherche Scientifique" and by the "Fonds National Suisse de la Recherche Scientifique".

REFERENCES

[1] Bondeson A., Manheimer W.M. and Ott E., Int. J. Infrared and Millimeter Waves **9**, 309 (1984)
[2] Perrenoud A., Tran T.M., Tran M.Q., Rieder C., Schleipen M. and Bondeson A., Int. J. of Electronics **57**, 985 (1984)
[3] Perrenoud A., Tran M.Q., Isaak B., Int. J. Infrared and Millimeter Waves **7**, 427 (1986)
[4] Sprangle P., Vomvoridis J.L., and Manheimer W.H., Physical Review A **23**, 3127 (1981)
[5] Open Resonators and Open Waveguides, Weinstein, L.A. Golem Series 1969
[6] Diffraction Loss and Selection of Modes in Maser Resonators with Circular Mirrors, Tingyi Li, The Bell System Technical Journal, 917 (1965)
[7] Conference Digest, 11th Int. Conference on Infrared and Millimeter Waves, Pisa (1986)
[8] Fliflet A.W., Reed M.E., Chu R.R. and Seeley R., Int. J. Electronics **53**, 505 (1982)

FIGURE CAPTIONS

Fig. 1 Resonator configuration with B_0 the magnetic field in the z-direction, d the mirror separation,a the mirror radius and $\delta y(x,z)$ the deviation from the underlying spherical surface

Fig. 2
a) Axonometric representation of a spherical mirror with R=720mm and a=200mm corresponding to a g-factor of g=±.5 for d=360mm
b) Axonometric representation of ellipsoidal mirror corresponding to g_z=+.5, g_x=-.5.
c) Axonometric representation of asymmetric mirror corresponding to g_z=+.5, g_x-.5

Fig. 3 Contour plot of diffraction losses as function of g_x and g_z for ellipsoidal mirrors.

Fig. 4 Contour plot of diffraction losses as function of the g-factor of the underlaying spherical surface and the deviation parameters s_z such that g_z-=g+2s_z.

Fig. 5 Contour plot of E-field maximum in the beam plane for asymmetric mirrors.

Fig. 6 Contour plot of E-field maximum as function of g_x and g_z for ellipsoidal mirrors.

Fig. 7 a) and b)
Contour plot of E-field in beam plane for spherical resonators with 4% diffraction losses (d=500mm). E-field maximum on mirror is normalized to one.

Fig. 8 a) and b)
Electronic efficiency contour plots for spherical mirrors

Fig. 9 a) and b)
Contour plots of electronic efficiency and E-field maximum for ellipsoidal mirrors in a scan g_x=-g_z.

Fig. 10 a) and b)
Contour plots of electronic efficiency and E-field maximum beam plane for asymmetric mirrors in a diagonal scan along unstability ridge (d=500mm).

Fig. 11 Contour plots of electronic efficiency and E-field maximum in beam plane for asymmetric mirrors (d=300mm).

Fig. 12 Contour plots of electronic efficiency for spherical resonators with output coupling slots
d=360mm, mirror radius = 70mm, outer slot radius = 43.5mm.

Fig. 13 a) and b)
Contour plots of electronic efficiency and E-field maximum for elliptical resonators with output coupling slots d=360mm, g_z=0, e.g. confocal in z-direction.

Fig. 14 a) through g)
Electronic output coupling, total efficiency and E-field maximum as function of the g-factor for spherical, ellipsoidal, asymmetric mirrors with 4% diffraction losses.

Fig. 15 a) and b)
Electronic output coupling and total efficiency and E-field maximum for spherical mirrors with different maximal heat load as function g
P_{max} (brass) = 1.1 kW/cm^2
P_{max} (brass) = 1.5 kW/cm^2
P_{max} (brass) = 1.5 kW/cm^2

Fig. 16 a) and b)
Electronic output coupling and total efficiency and E-field maximum for spherical mirrors with 10% and 20% diffraction losses.

Material	Conductivity	Max E-field yielding 1.5kW/cm^2	Max E-field yielding 1.1kW/cm^2
Copper	$5.8 \cdot 10^7 \Omega^{-1}m^{-1}$	3.43MV/m	2.94MV/m
Brass	$1.4 \cdot 10^7 \Omega^{-1}m^{-1}$	2.405MV/m	2.059MV/m
Brass	$0.86 \cdot 10^7 \Omega^{-1}m^{-1}$ (anomalous conductivity)	2.13MV/m	1.78MV/m

Table 1

Maximum permissible electric field on the mirror under the condition of a maximum permissible heat load

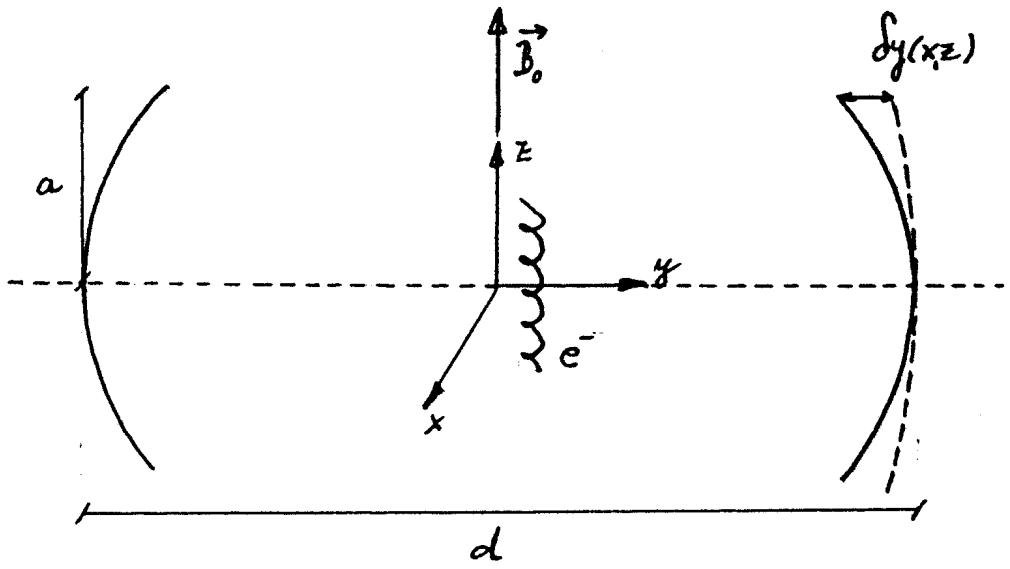

Figure 1

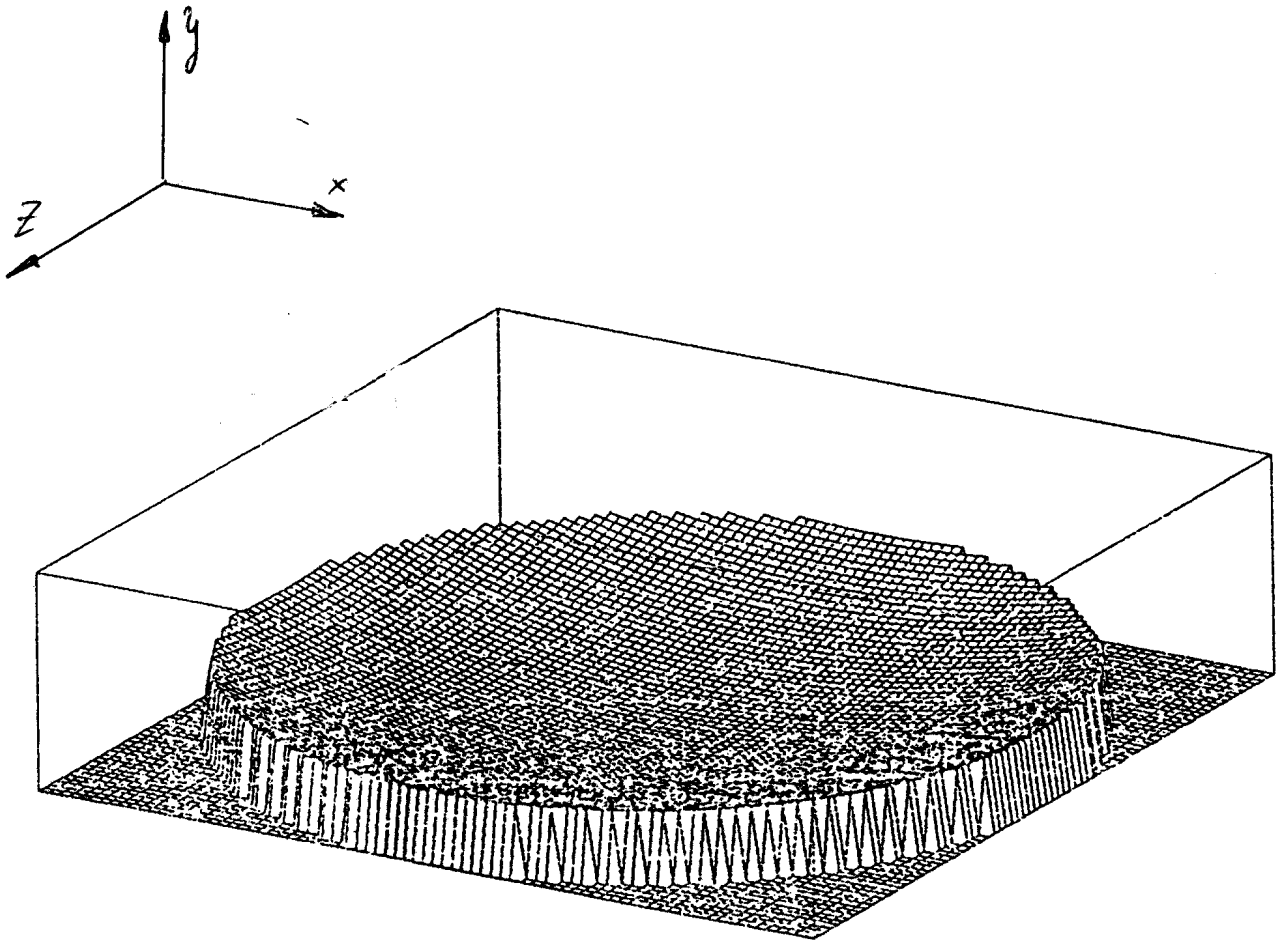

Figure 2a

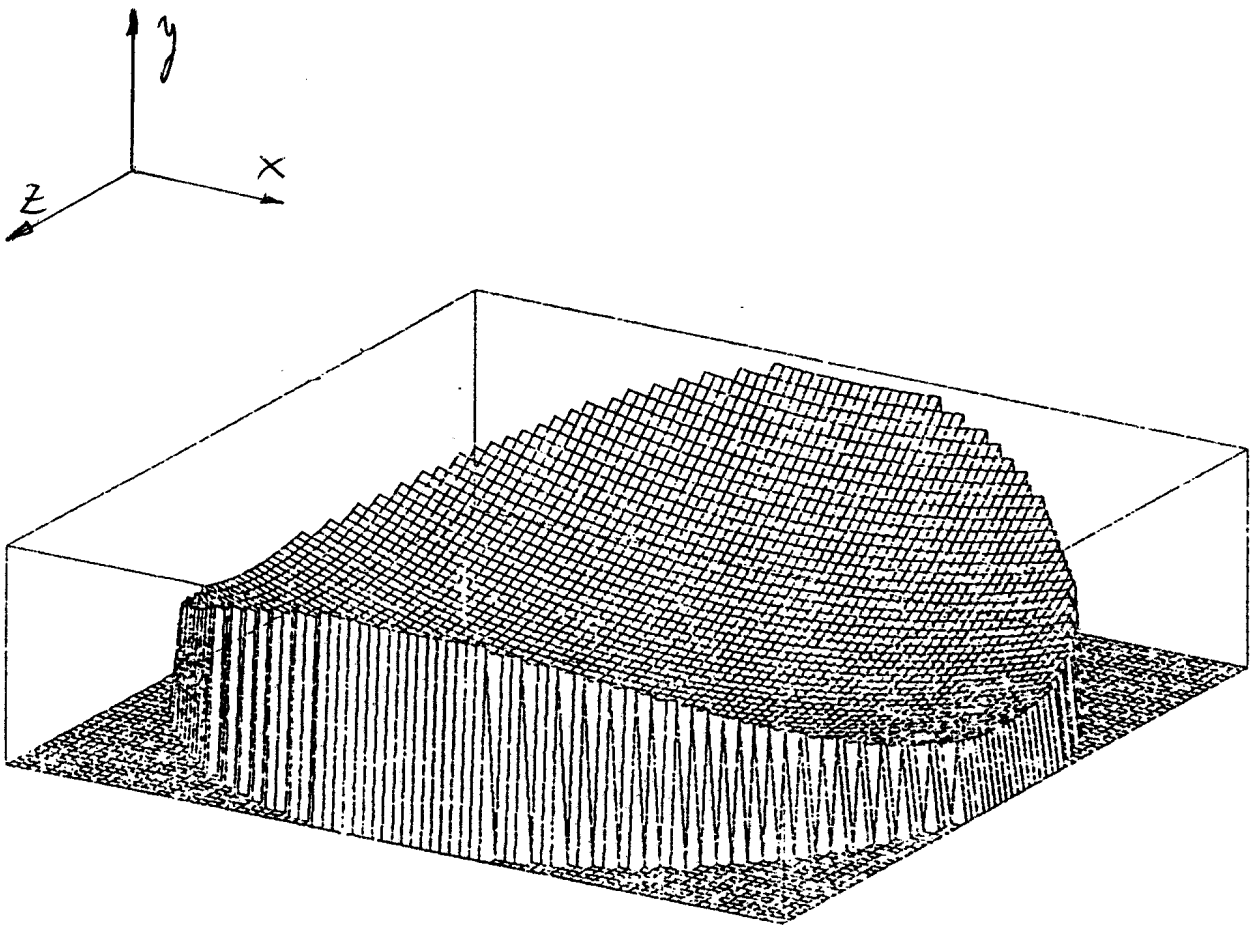

Figure 2b

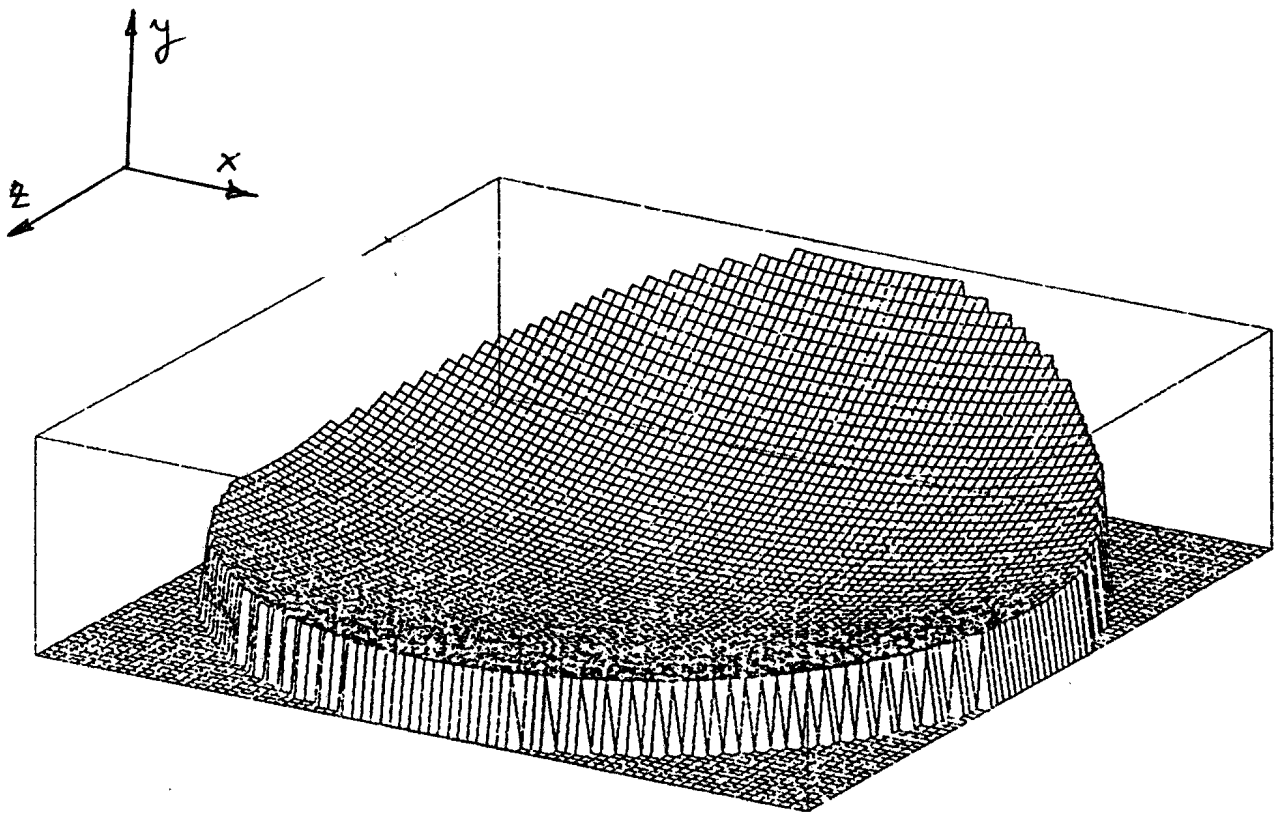

Figure 2c

Ellipsoidal mirrors

Total diffraction losses T(2-way losses)

d = 360 mm

a = 30 mm

λ = 2.5 mm

$N = a^2/\lambda d = 1$

$T_{min} = 0.001$

$T_{max} = 0.379$

separation of contour lines = 0.01

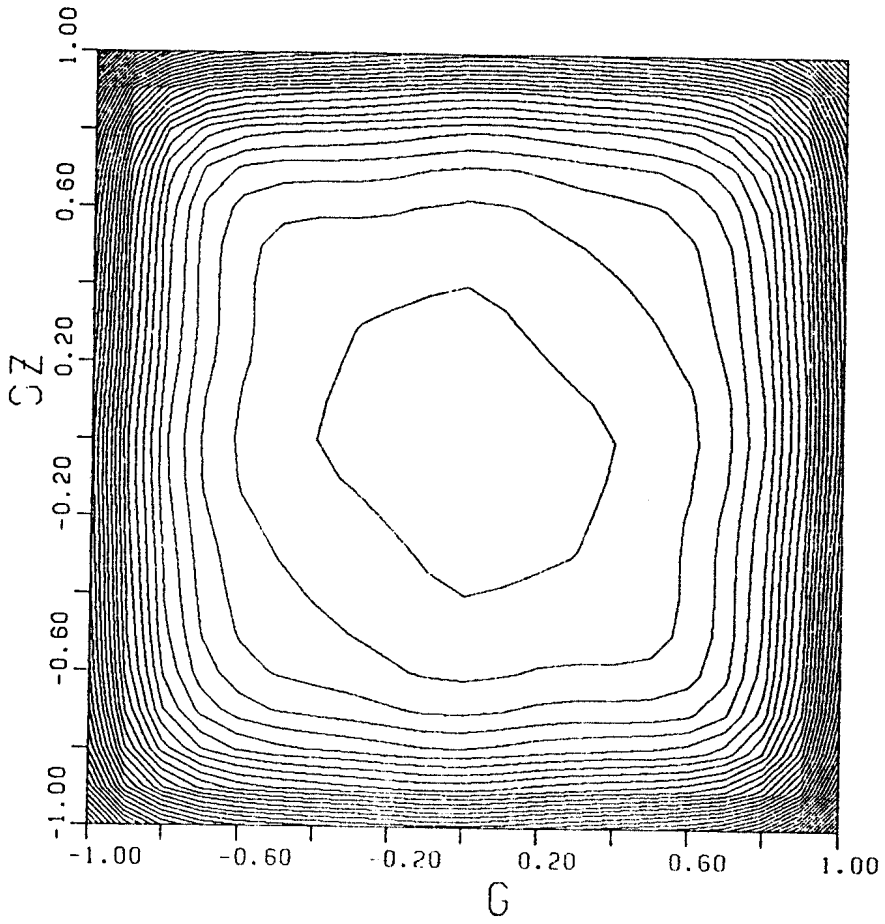

Figure 3

Asymmetric mirrors

Total diffraction losses T (2-way losses)

d = 360 mm

a = 30 mm

λ = 2.5 mm

$N = a^2/\lambda d = 1$

$T_{min} = 0.001$

$T_{max} = 0.807$

separation of contour lines = 0.02

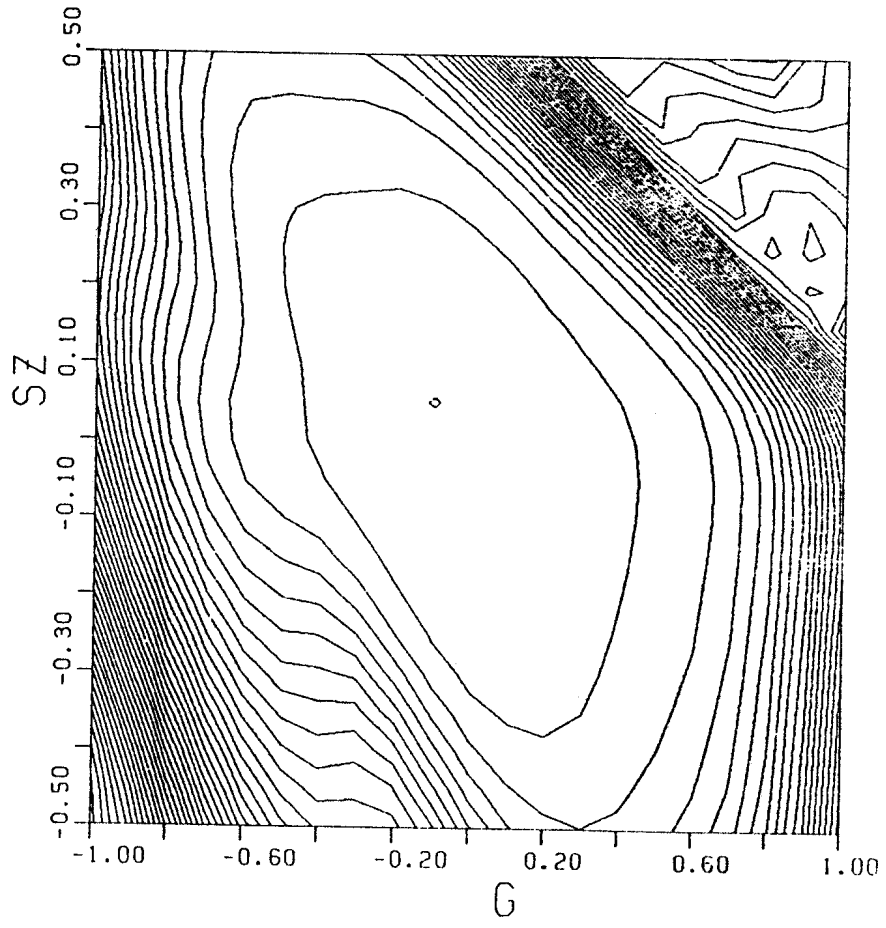

Figure 4

Asymmetric mirrors

normalized E-field in beam plane (maximum field value on mirrors normalized to 1)

d = 360 mm

a = 30 mm

λ = 2.5 mm

E_{min} = 0.86

E_{max} = 4.23

separation of contour lines = 0.07

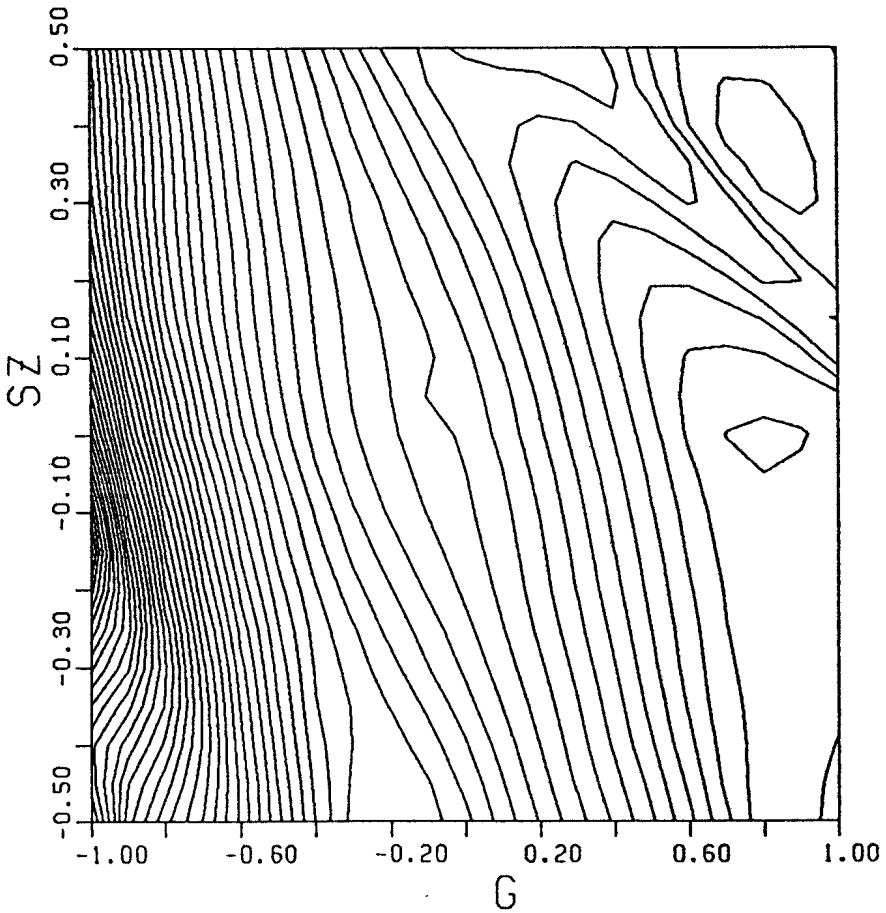

Figure 5

Ellipsoidal mirrors

normalized E-field in beam plane (maximum field value on mirrors normalized to 1)

d = 360 mm

a = 30 mm

λ = 2.5 mm

E_{min} = 0.89

E_{max} = 3.67

separation of contour lines = 0.06

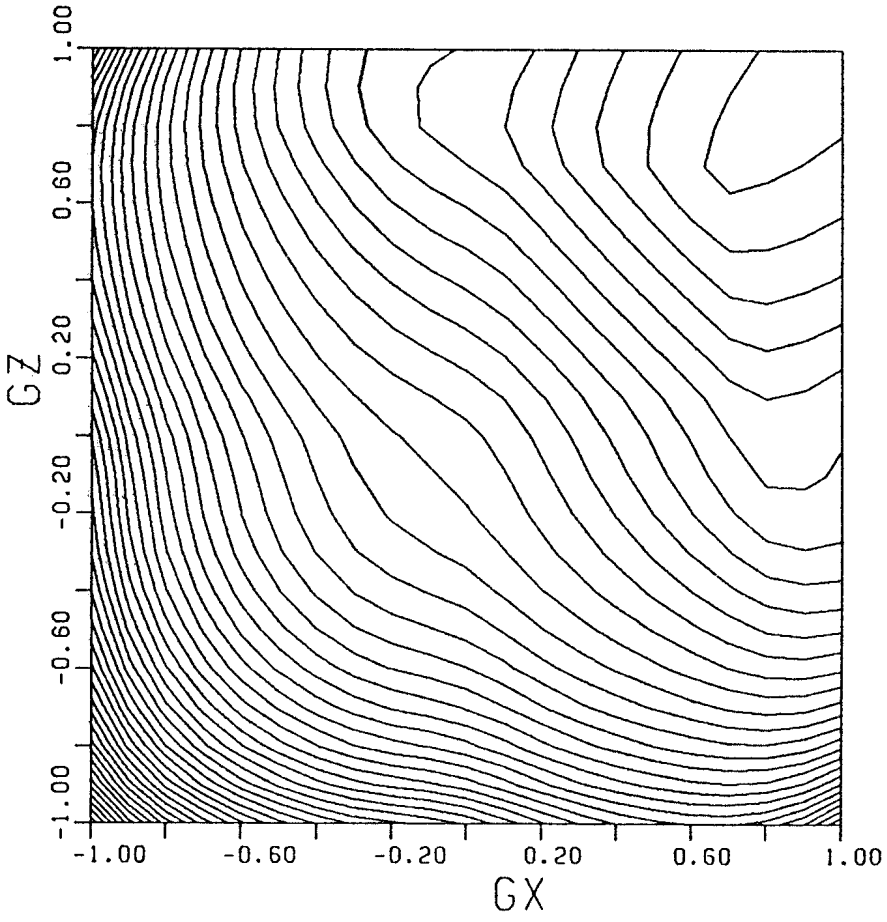

Figure 6

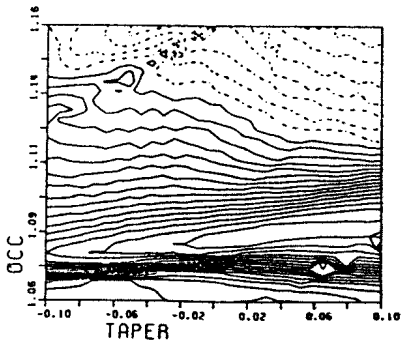

g = -.9
max = .53

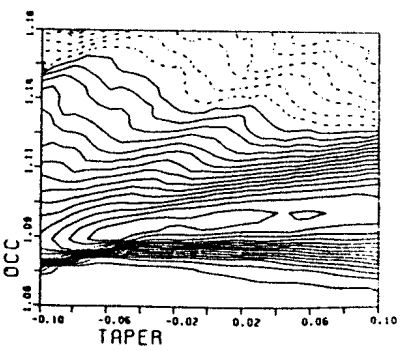

g = -.8
max = .46

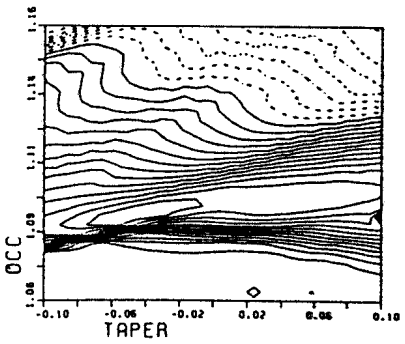

g = -.7
max = .44

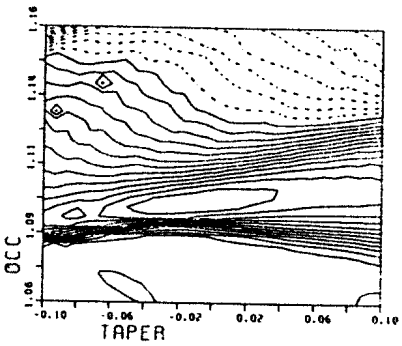

g = -.6
max = .42

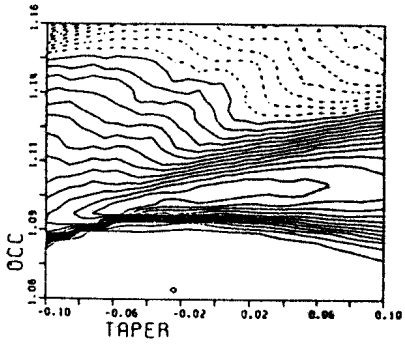

g = -.5
max = .40

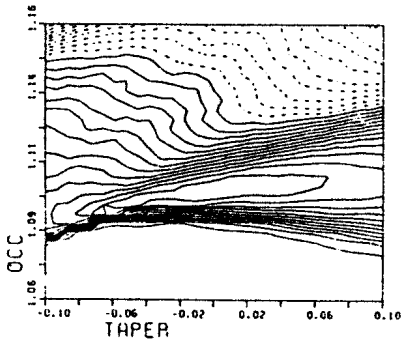

g = -.4
max = .39

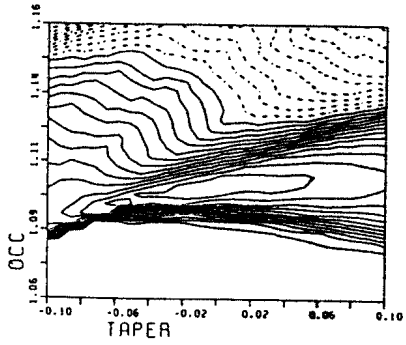

g = -.3
max = .39

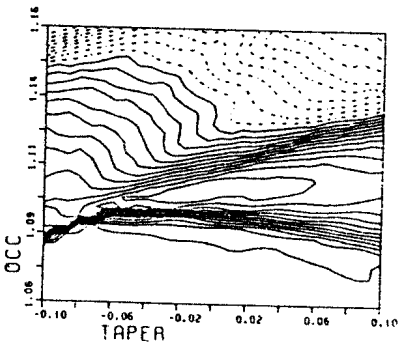

g = -.2
max = .39

Figure 7a

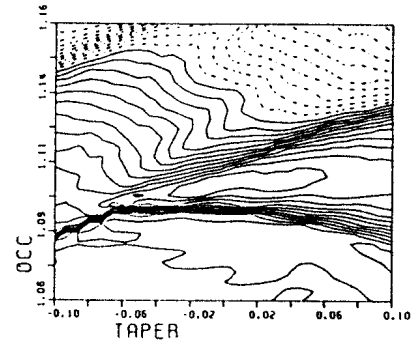

g = -.1
max = .38

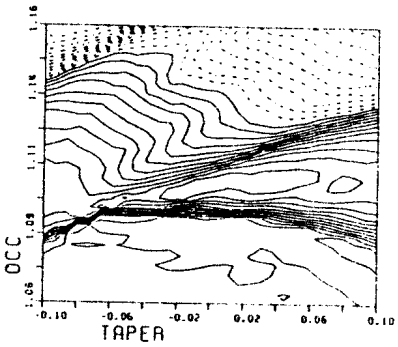

g = .0
max = .38

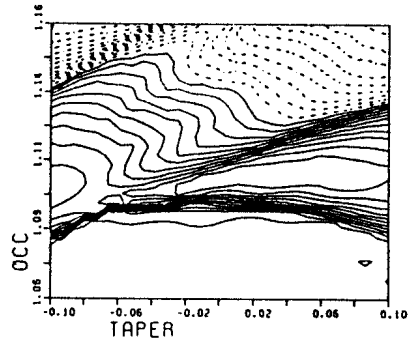

g = +.1
max = .37

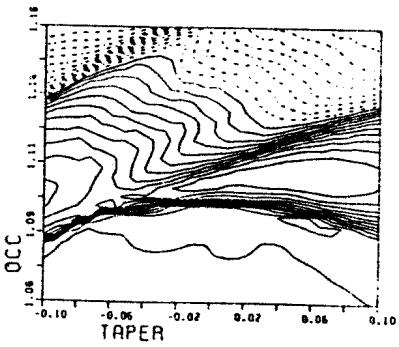

g = +.2
max = .36

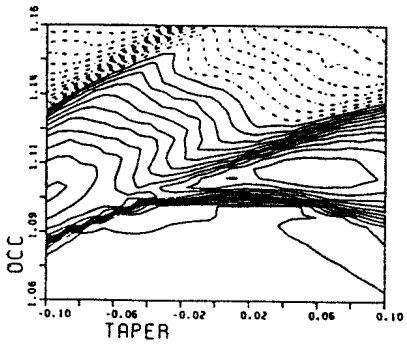

g = +.3
max = .35

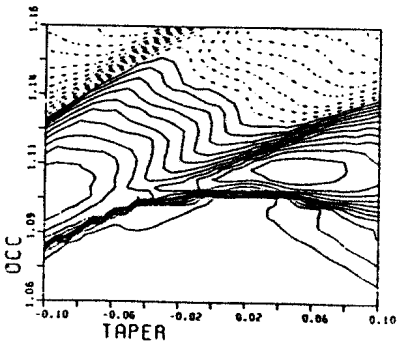

g = +.4
max = .35

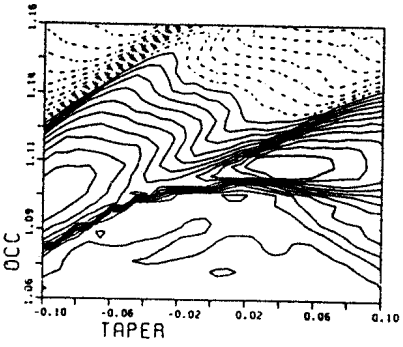

g = +.5
max = .34

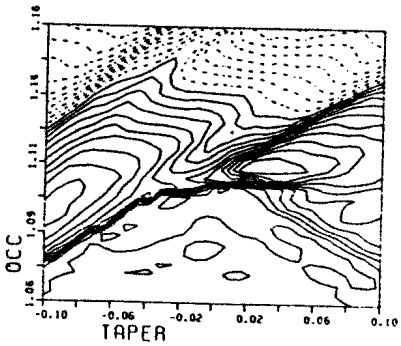

g = +.6
max = .34

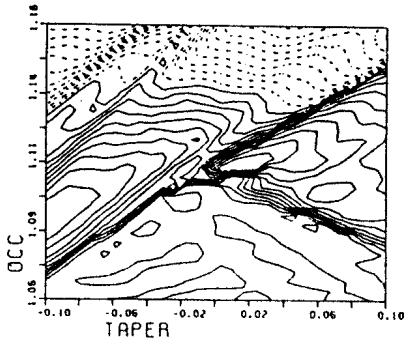

g = +.7
max = .35

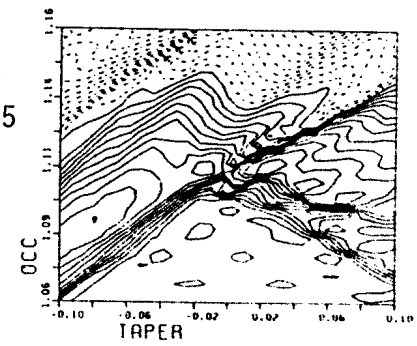

g = +.8
max = .37

Figure 7b

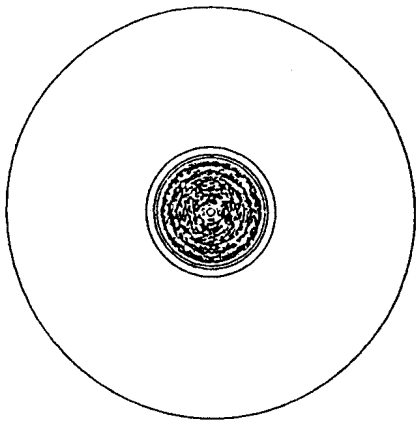

g = -.9
a = 46 mm
e-max = 4.2

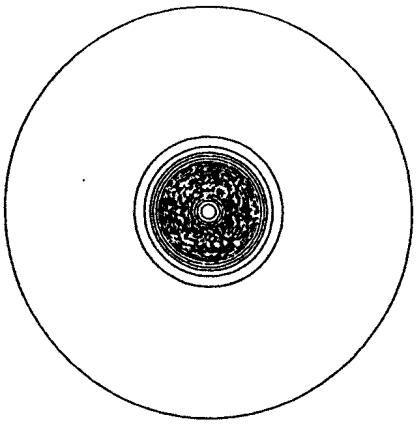

g = -.8
a = 41 mm
e-max = 2.8

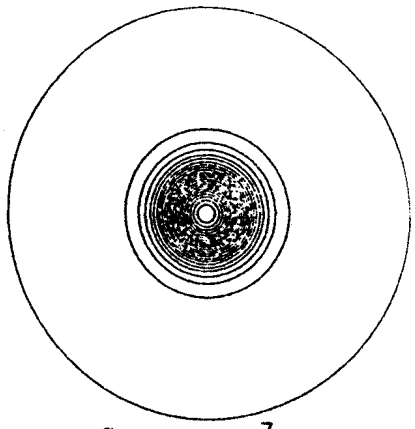

g = -.7
a = 37 mm
e-max = 2.3

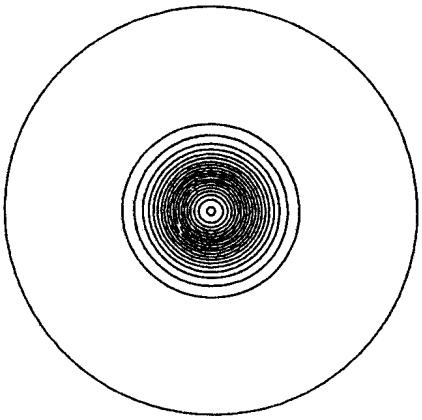

g = -.6
a = 35 mm
e-max = 2.1

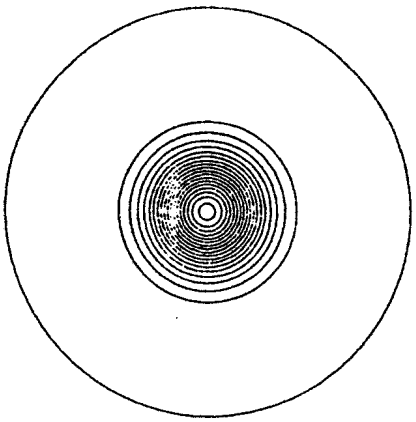

g = -.5
a = 34 mm
e-max = 1.9

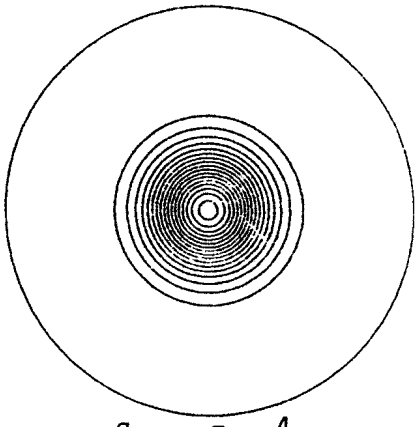

g = -.4
a = 39 mm
e-max = 1.8

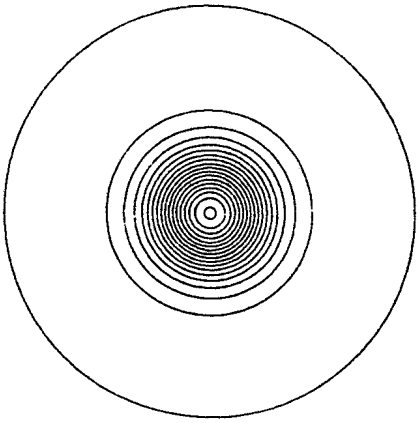

g = -.3
a = 31 mm
e-max = 1.8

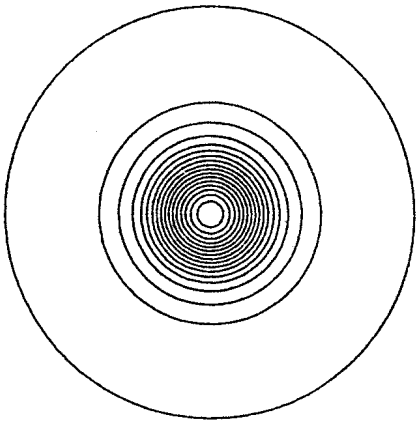

g = -.2
a = 30 mm
e-max = 1.7

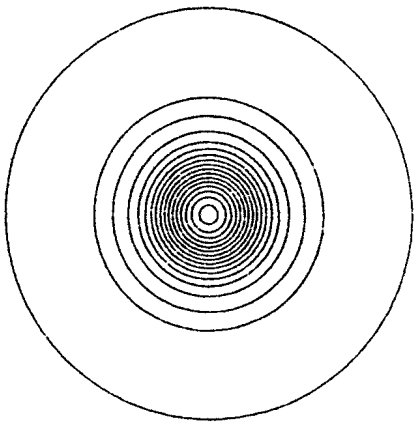

g = -.1
a = 29 mm
e-max = 1.7

Figure 8a

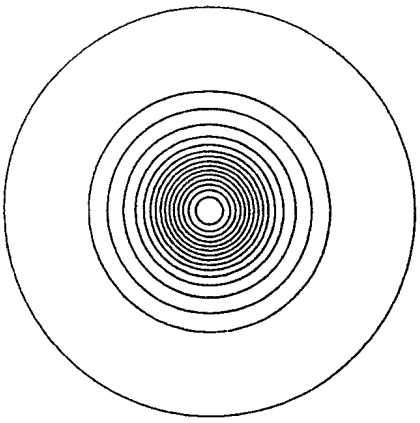

g = 0 e-max = 1.6
a = 29 mm

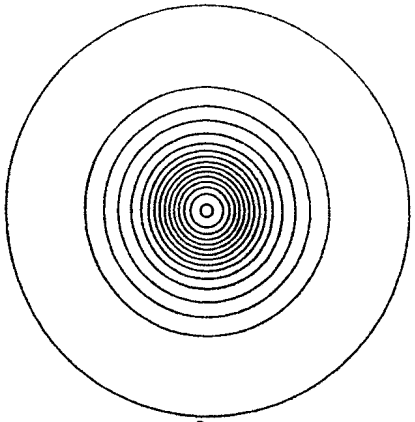

g = +.1 e-max = 1.6
a = 29 mm

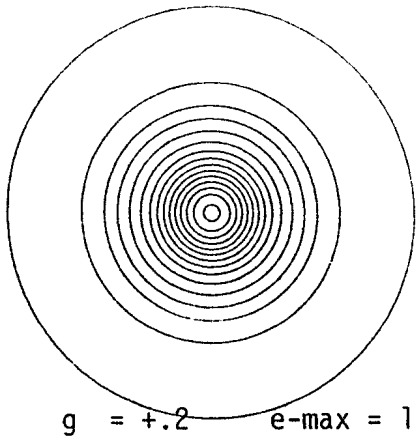

g = +.2 e-max = 1.5
a = 30 mm

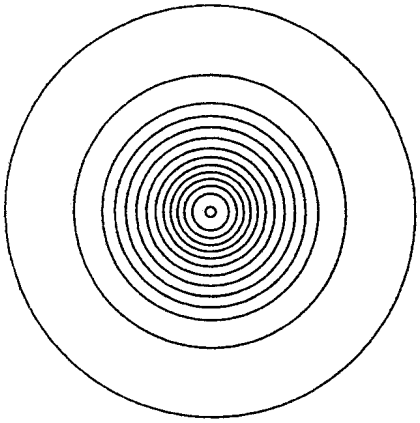

g = +.3 e-max = 1.4
a = 31 mm

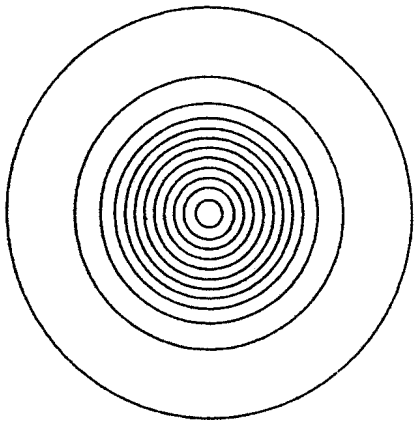

g = +.4 e-max = 1.2
a = 33 mm

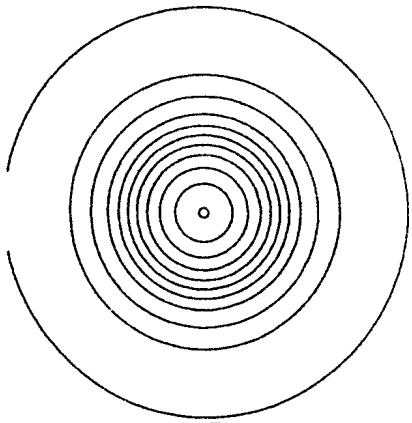

g = +.5 e-max = 1.
a = 34 mm

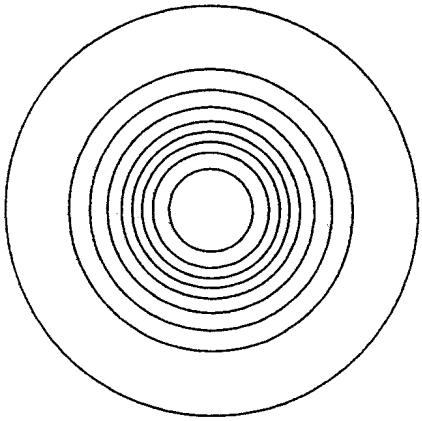

g = +.6 e-max = 0.9
a = 35mm

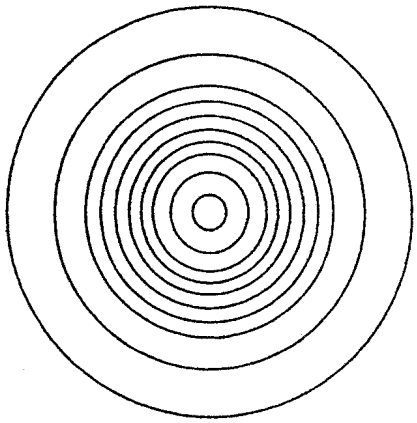

g = +.7 e-max = 0.9
a = 37 mm

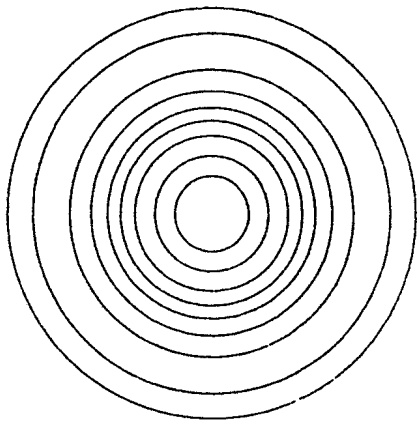

g = +.8 e-max = 0.
a = 41 mm

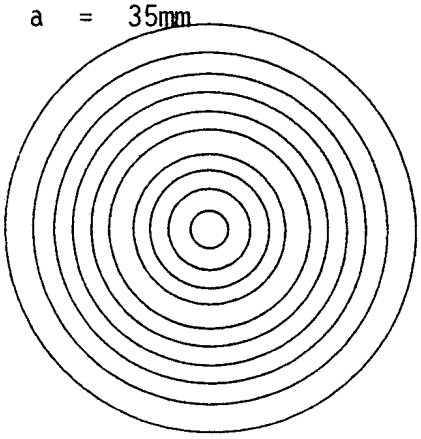

g = +.9 e-max = 1.1
a = 47 mm

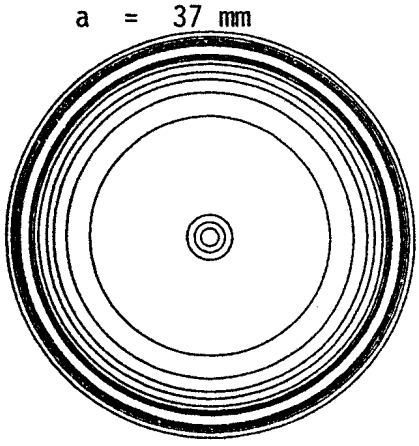

g = 1. e-max 1.2
a = 73 mm

Figure 8b

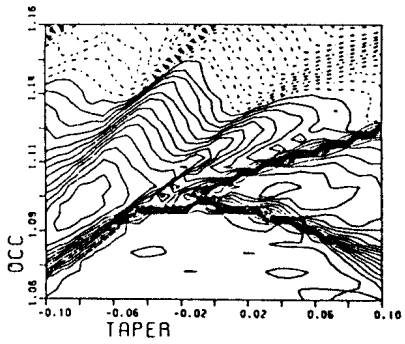

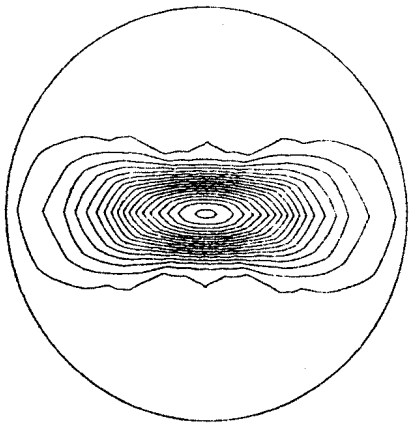

g_x = -.8 max = .48

g_z = +.8 e-max = 1.9

a = 40 mm

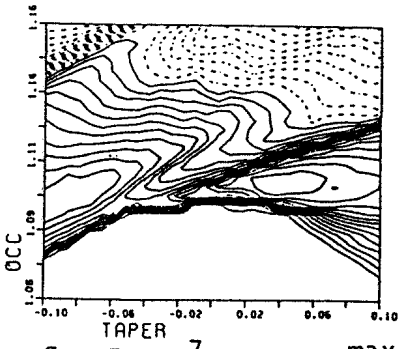

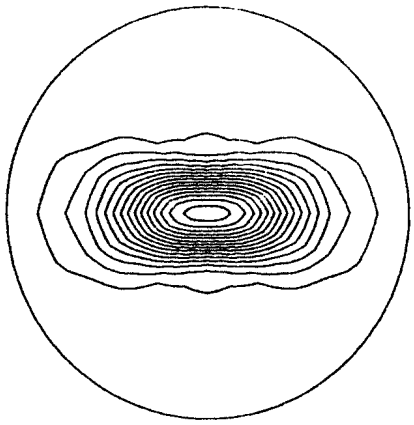

g_x = -.7 max = .45

g_z = +.7 e-max = 1.6

a = 36 mm

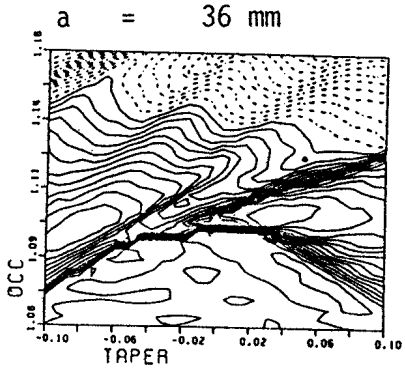

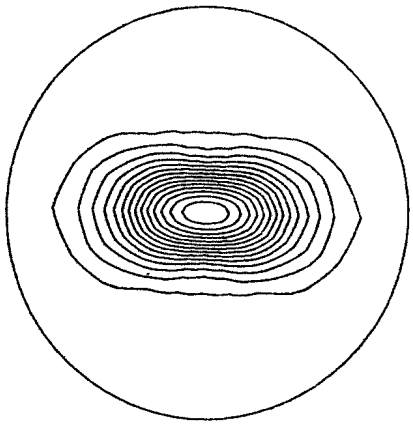

g_x = -.6 max = .43

g_z = +.6 e-max = 1.5

a = 34 mm

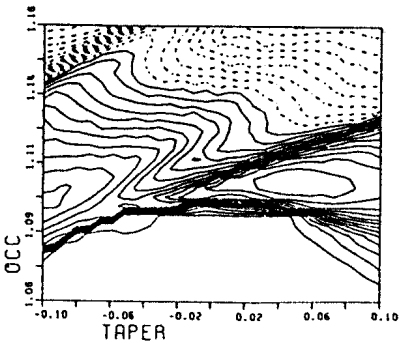

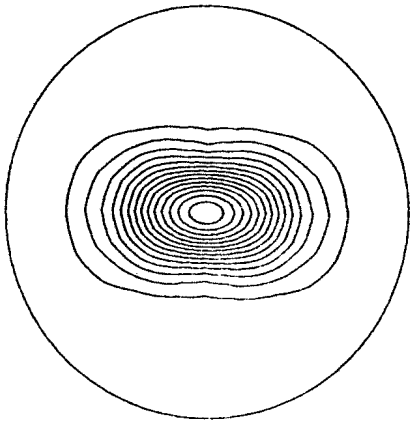

g_x = -.5 max = .40

g_z = +.5 e-max = 1.5

a = 33 mm

Figure 9a

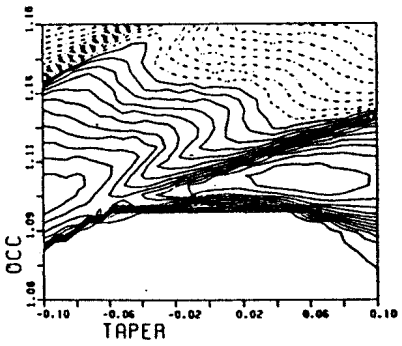

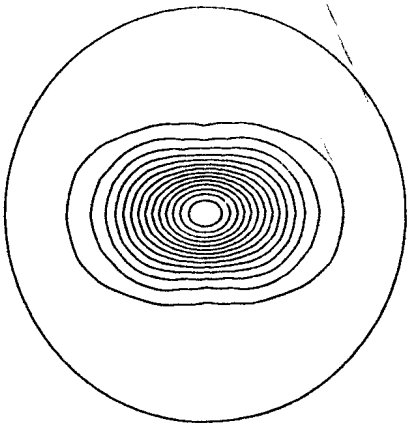

g_x = -.4 max = .40

g_z = +.4 e-max = 1.5

a = 30 mm

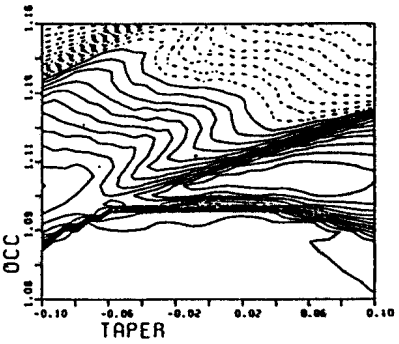

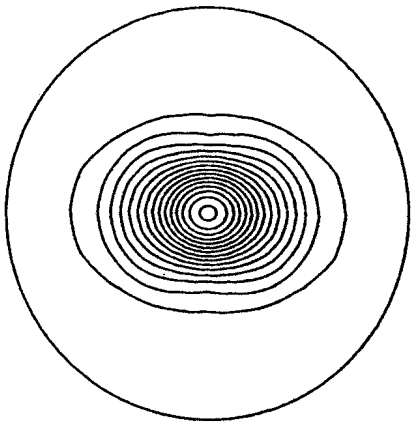

g_x = -.3 max = .38

g_z = +.3 e-max = 1.6

a = 31 mm

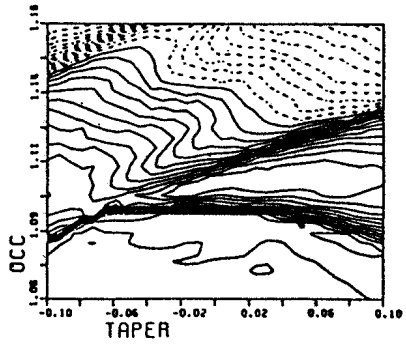

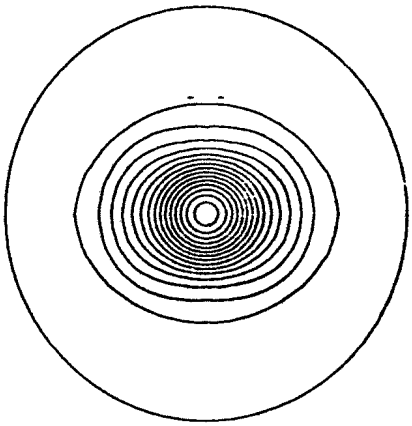

g_x = -.2 max = .37

g_z = +.2 e-max = 1.6

a = 30 mm

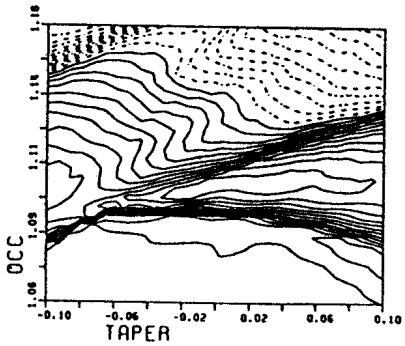

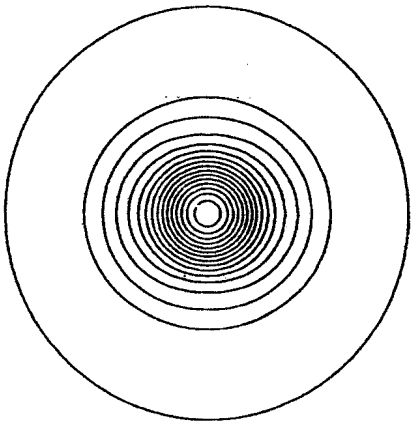

g_x = -.1 max = .38

g_z = +.1 e-max = 1.6

a = 29 mm

Figure 9b

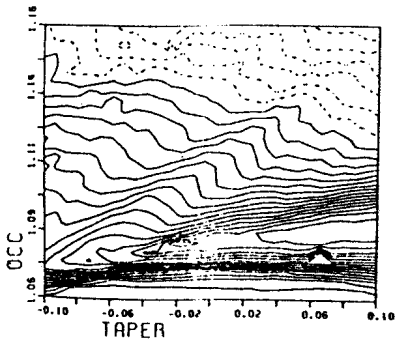

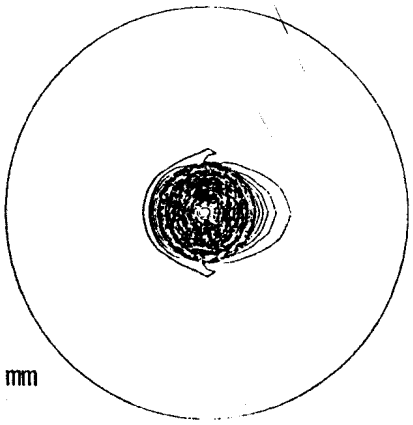

g = -.95 a = 49 mm

s_z = -.065 max = .50

g_z^* = -.82 e-field max = 4.6

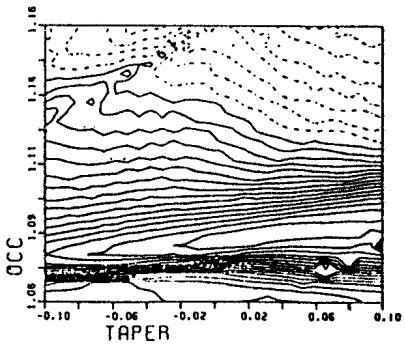

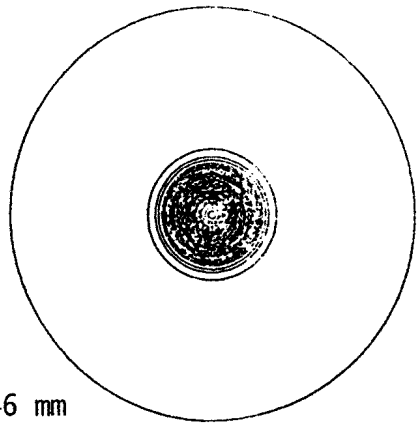

g = -.9 a = 46 mm

s_z = 0. max = .53

g_z^* = -.9 e-field max = 4.2

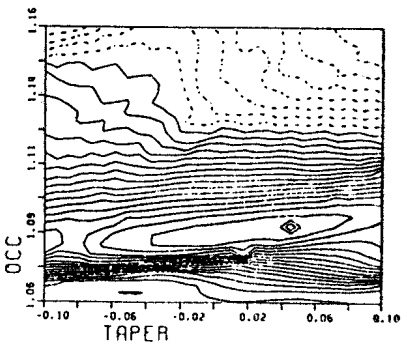

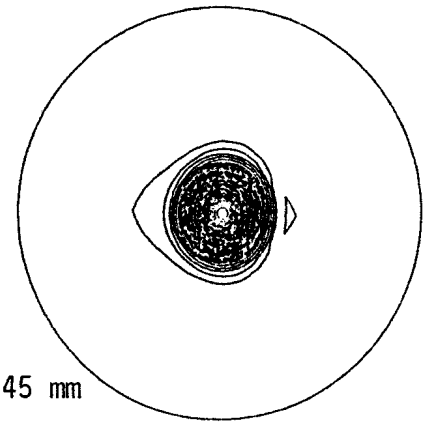

g = -.85 a = 45 mm

s_z = -.065 max = .56

g_z^* = -.98 e-field max = 3.8

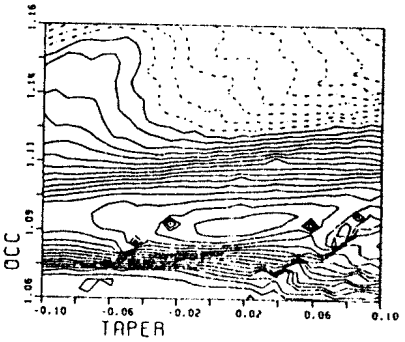

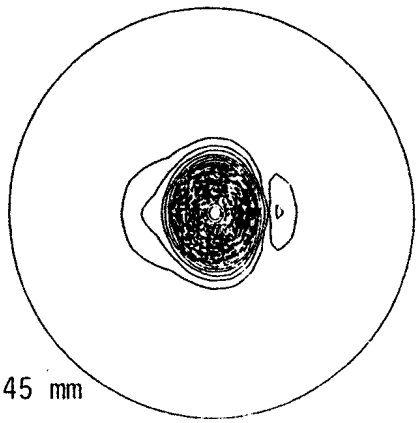

g = -.8 a = 45 mm

s_z = -.13 max = .56

g_z^* e-field max = 3.5

Figure 10a

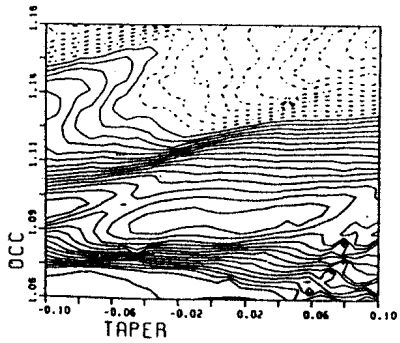

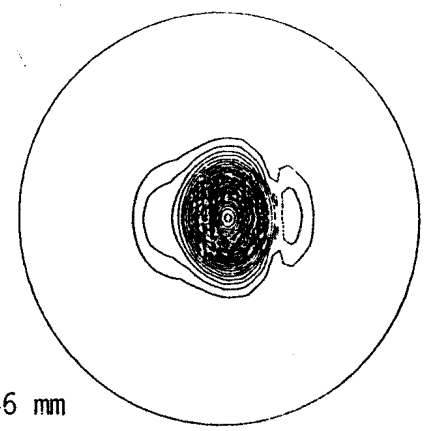

g = -.75 a = 46 mm

s_z = -.195 max = .46

g_z^* = -1.15 e-field max = 3.3

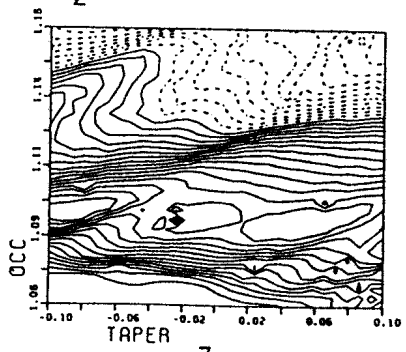

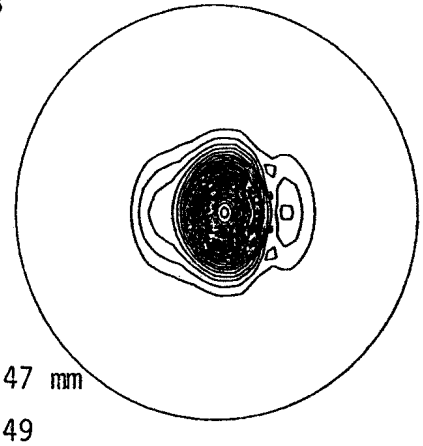

g = -.7 a = 47 mm

s_z = -.26 max = .49

g_z^* = -1.22 e-field max = 3.1

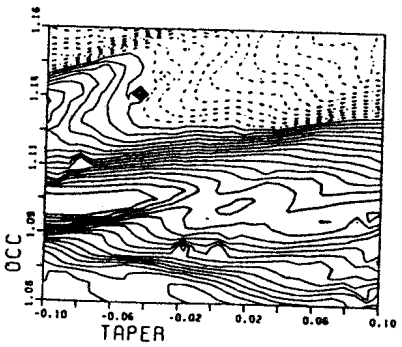

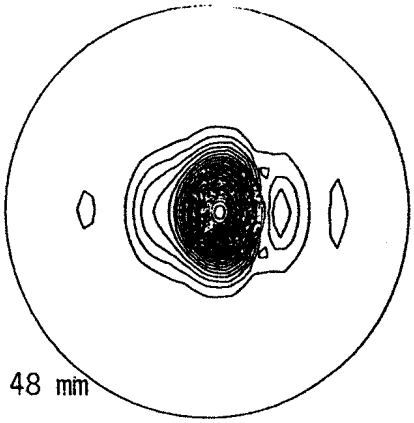

g = -.65 a = 48 mm

s_z = -.325 max = .48

g_z^* = -1.3 e-field max = 2.9

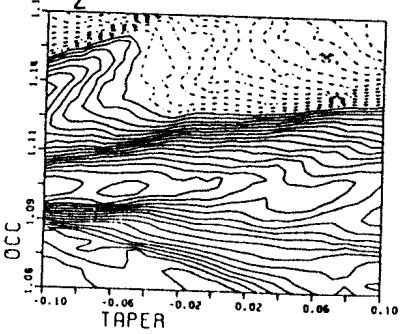

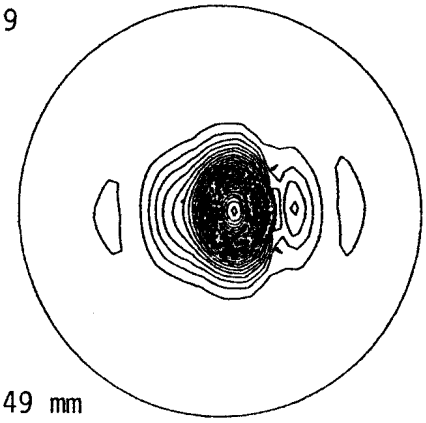

g = -.6 a = 49 mm

s_z = -.35 max = .48

g_z^* = -1.4 e-field max = 2.9

Figure 10b

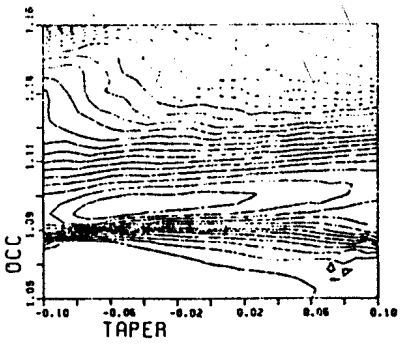

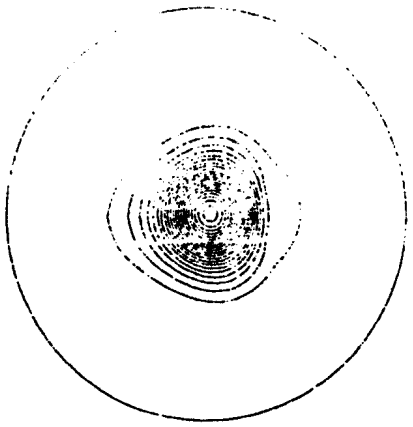

g = -.6 a = 31 mm

s_z = -.1 max = .42

g_z^* = -.8 e-max = 2.2

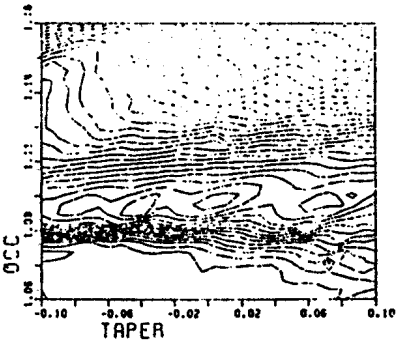

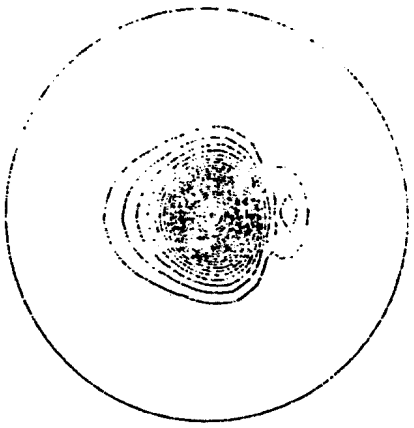

g = -.6 a = 35 mm

s_z = -.2 max = .46

g_z^* = -1.0 e-max = 2.4

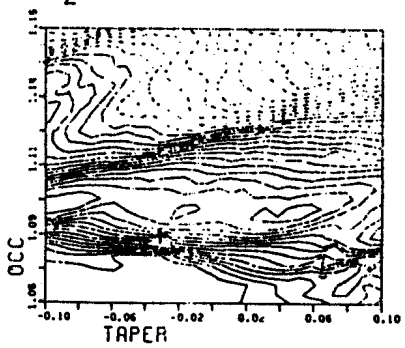

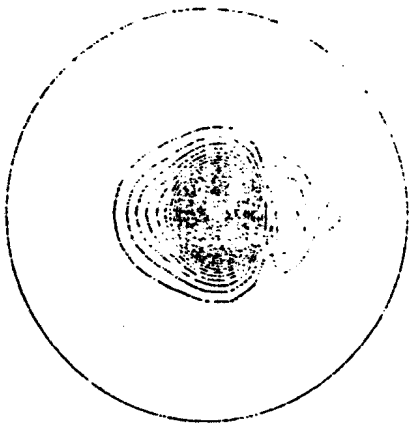

g = -.6 a = 38 mm

s_z = -.3 max = .44

g_z^* = -1.2 e-max = 2.5

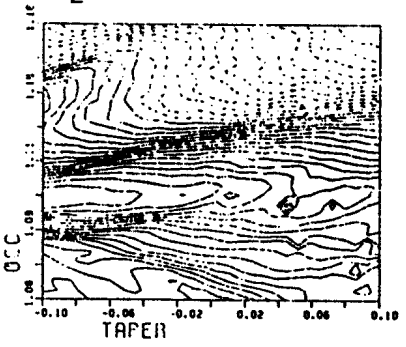

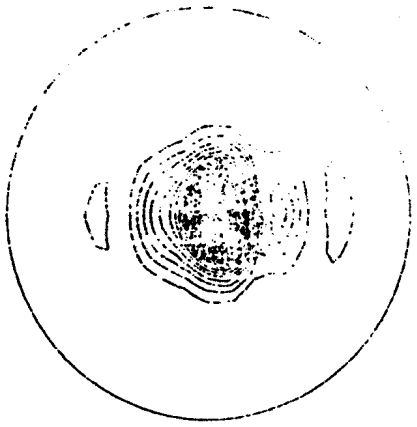

g = -.6

s_z = -.4 max = .48

g_z^* = -1.4 e-max = 2.6

Figure 11

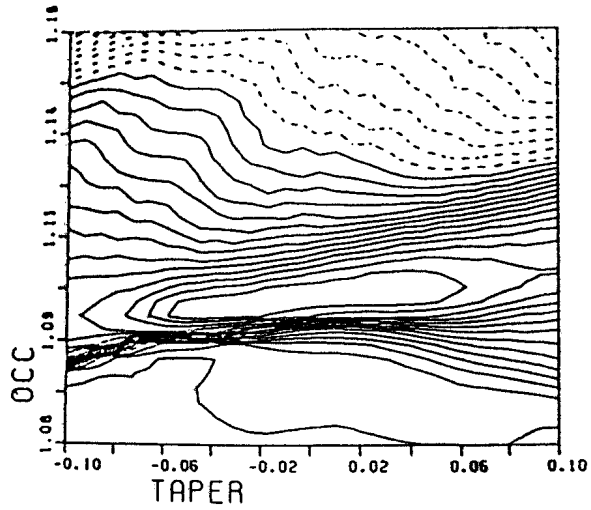

g = -.6
a = .30 mm
max = .44
ceff = .75 (.78)
teff = .34

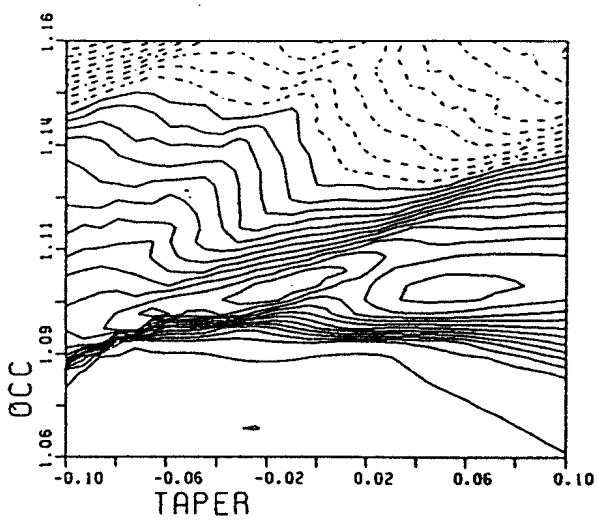

g = -.3
a = .27 mm
max = .39
ceff = .88 (.91)
teff = .35

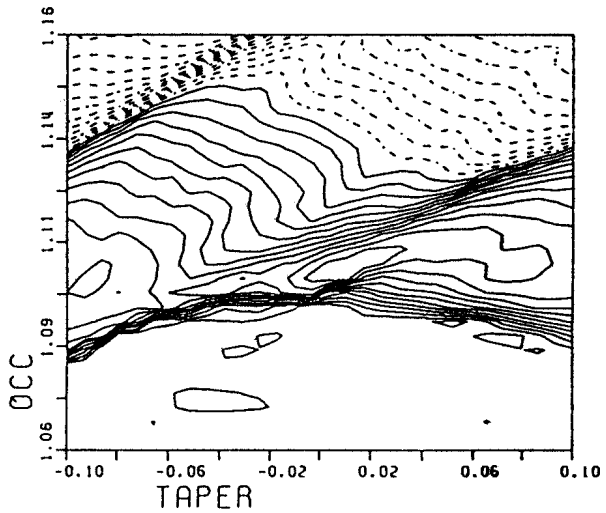

g = +.3
a = .26 mm
max = .37
ceff = .91
teff = .34

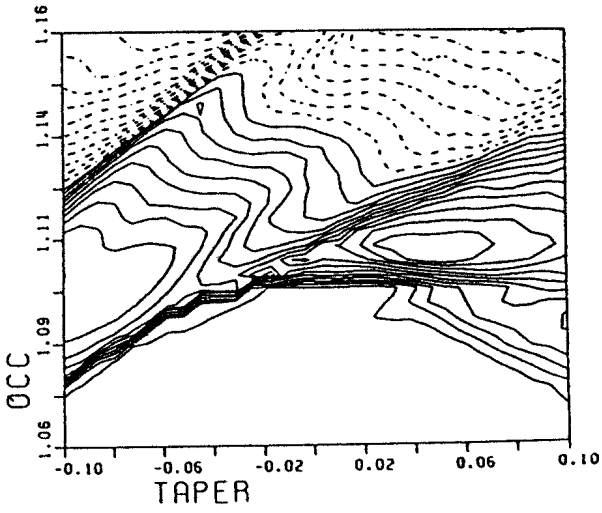

g = +.6
a = .30
max = .36
ceff = .78
teff = .28

Figure 12

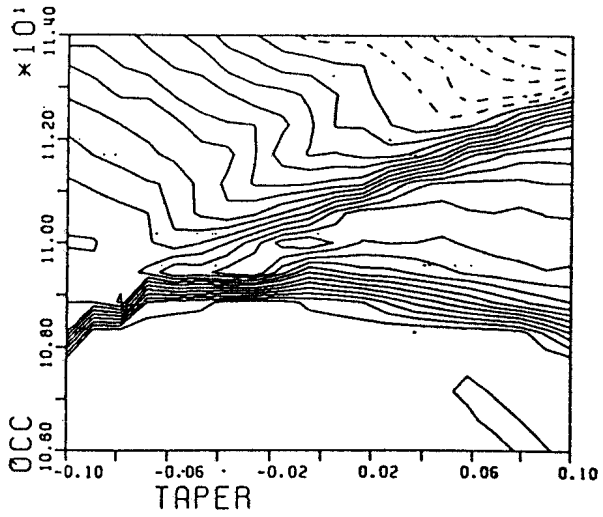

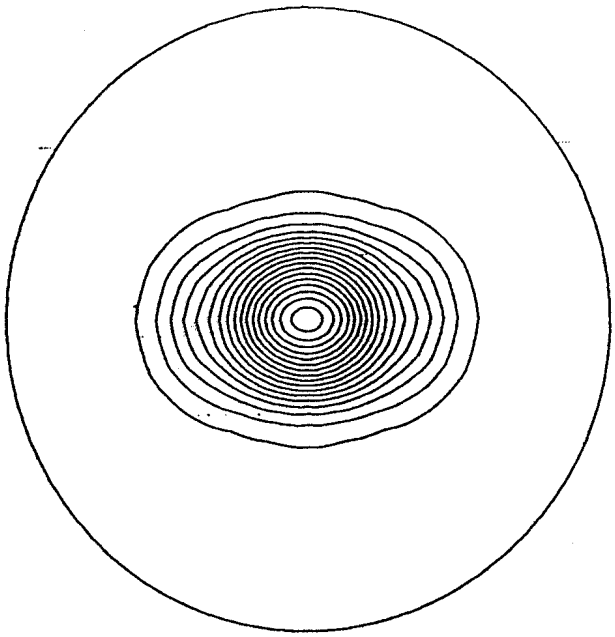

g_x = -.6 g_z^* = 0

a = 28 mm

max = .42

e-max = 1.8 , ceff = .77 , teff = .34

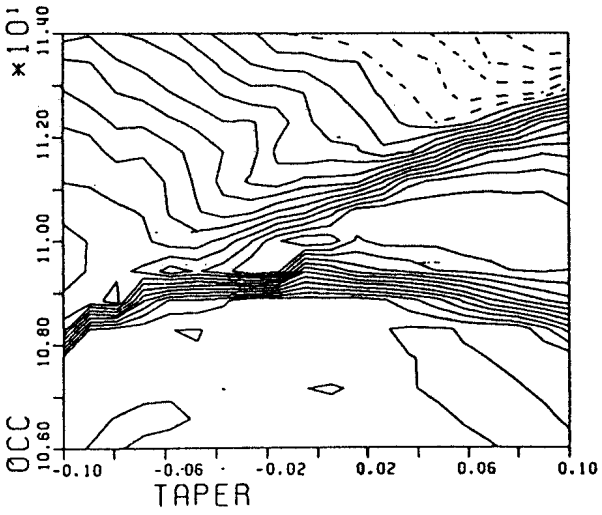

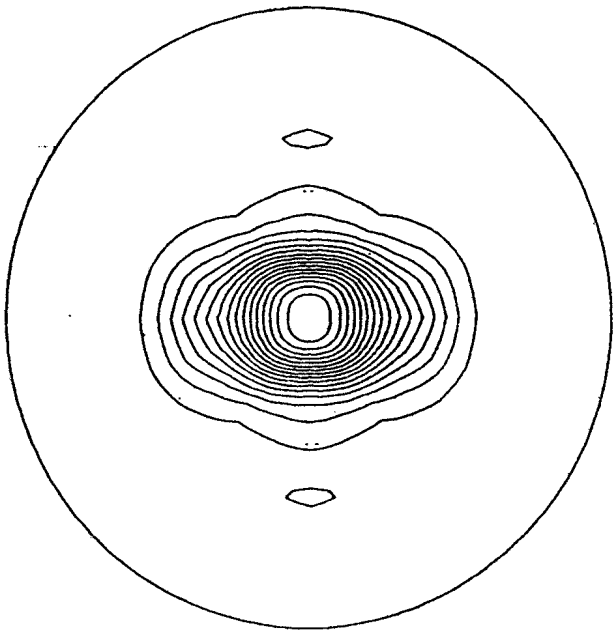

g_x = -.7 g_z^* = 0

a = 29 mm

max = .4

e-max = 1.7 , ceff = .69 , teff = .28

Figure 13a

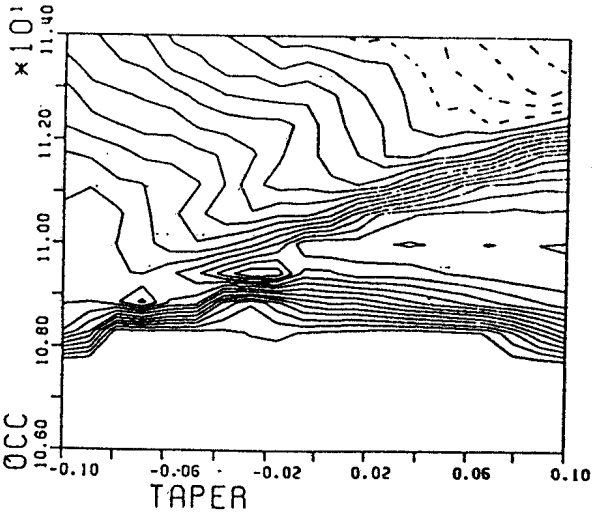

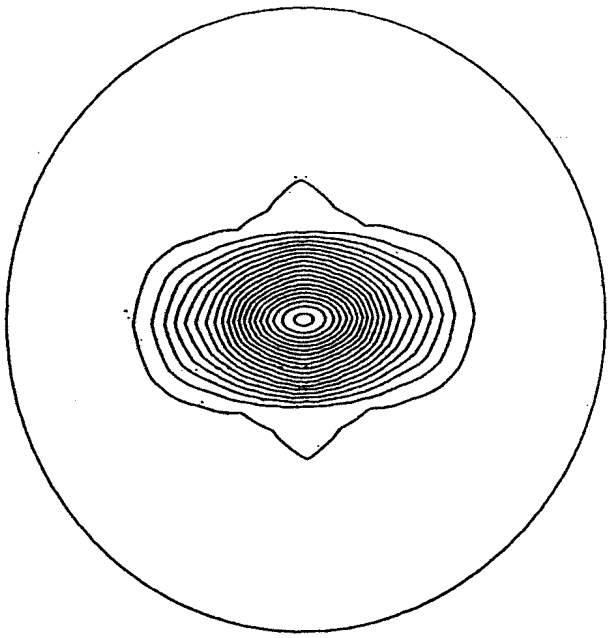

g_x = -.8 g_z^* = 0

a = 29 mm

max = .4

e-max = 2.1 , ceff = .64 , teff = .28

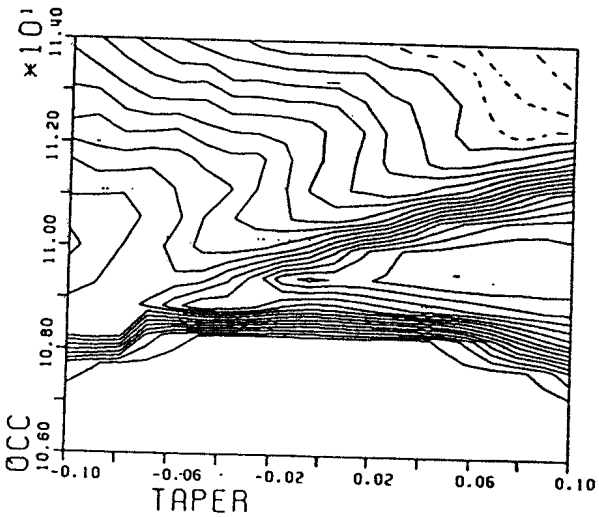

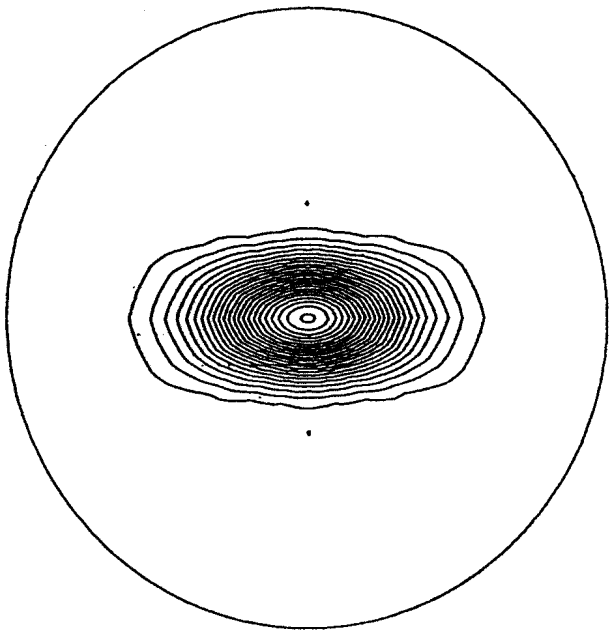

g_x = -.9 g_z^* = 0

a = 35 mm

max = .46

e-max = 2.4 , ceff = .64 , teff = .29

Figure 13b

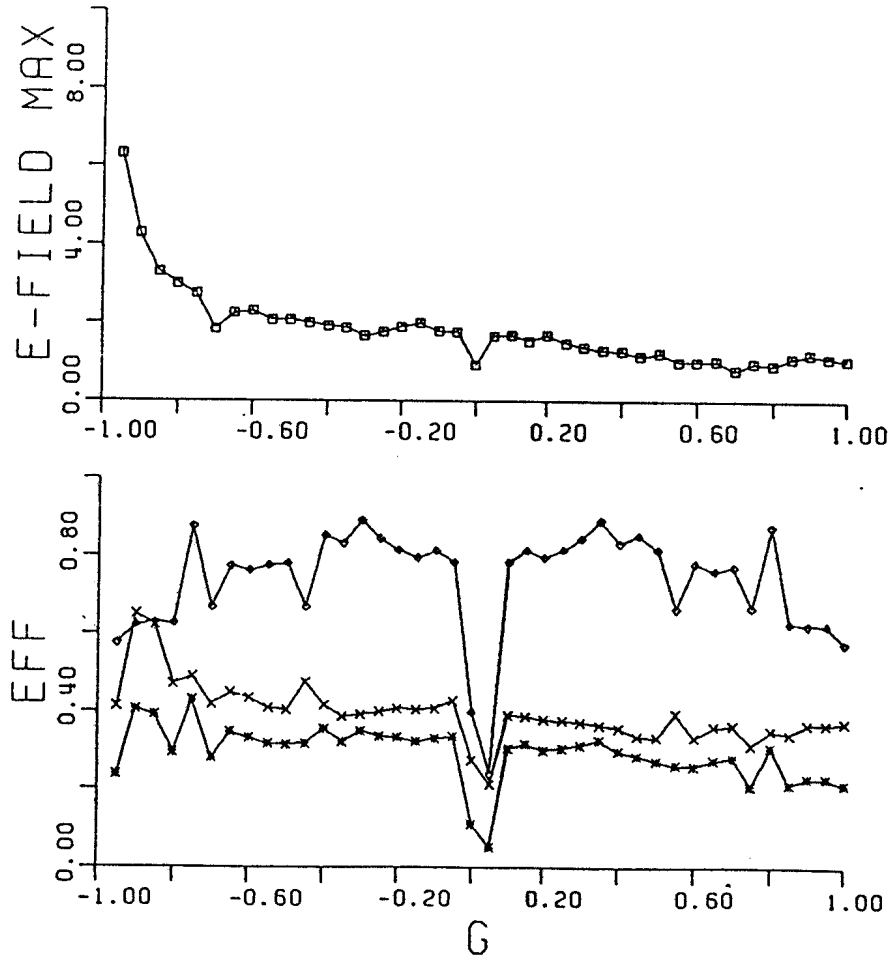

× ELECTRONIC EFFICIENCY

◇ OUTPUT COUPLING EFF

✱ TOTAL EFFICIENCY

□ E-FIELD MAX

SPHERICAL RESONATORS

4% DIFFFRACTION LOSS

Figure 14a

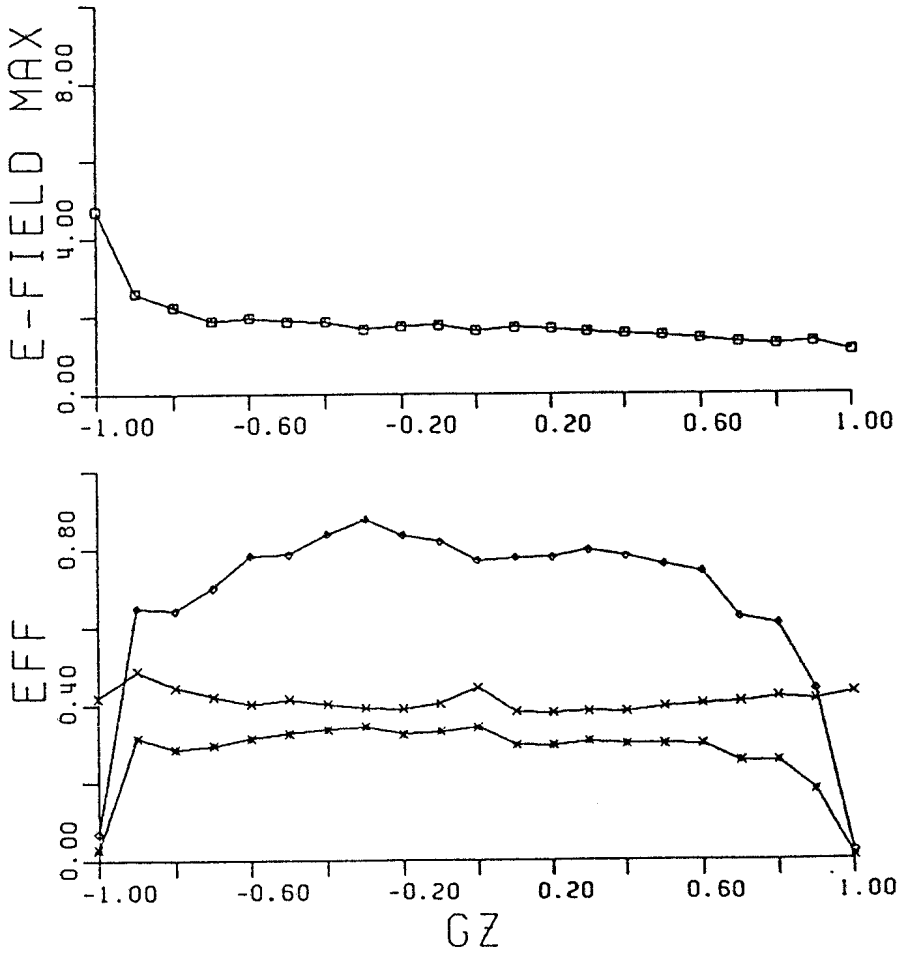

× ELECTRONIC EFFICIENCY

◇ OUTPUT COUPLING EFF

✱ TOTAL EFFICIENCY

□ E-FIELD MAX

ELLIPTICAL MIRRORS

GX=-.3

Figure 14b

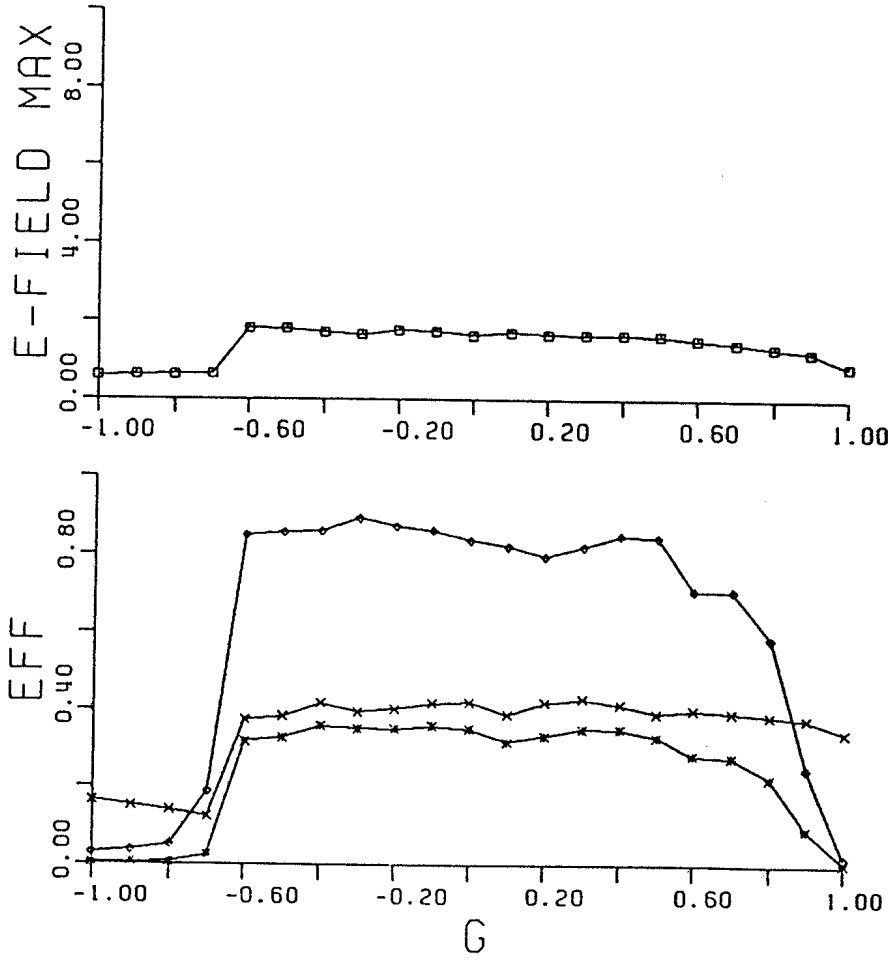
E-FIELD MAX
8.00
4.00
0.00
-1.00
-0.60
-0.20
0.20
0.60
1.00
EFF
0.80
0.40
0.00
-1.00
-0.60
-0.20
0.20
0.60
1.00
G
× ELECTRONIC EFFICIENCY
◆ OUTPUT COUPLING EFF
✱ TOTAL EFFICIENCY
▫ E-FIELD MAX
ASYMETRIC MIRRORS
GX=-.3
4% LOSSES

Figure 14c

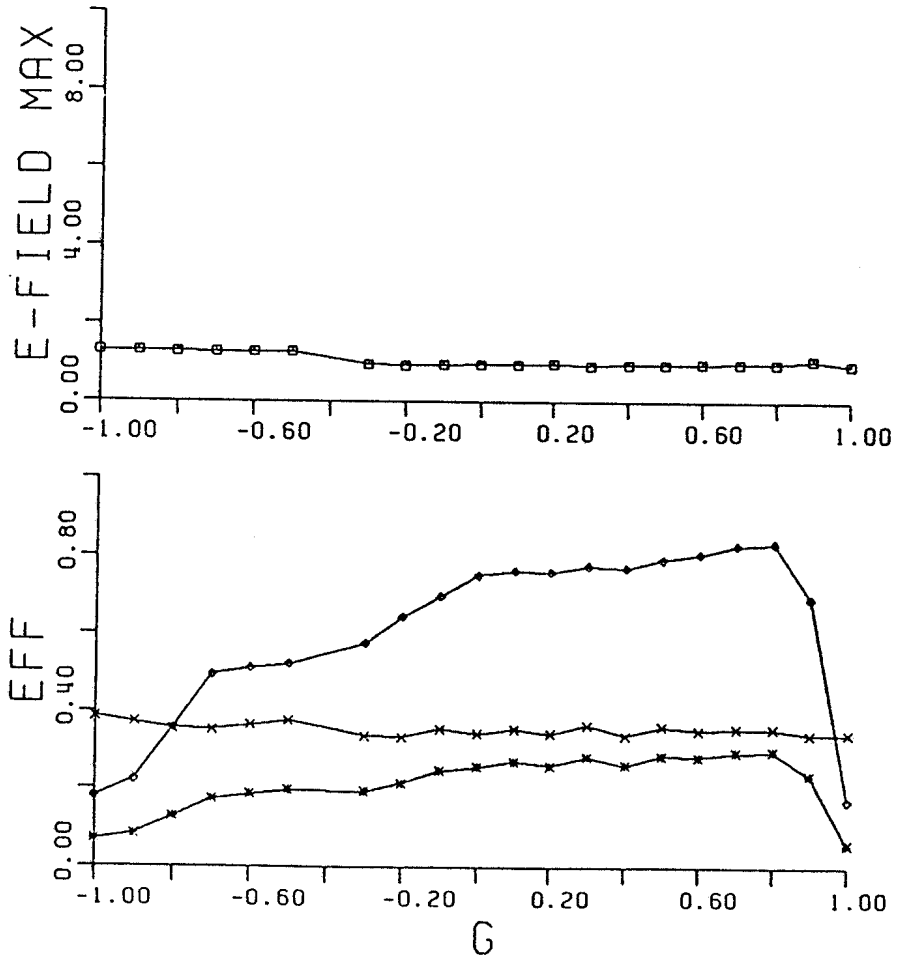

× ELECTRONIC EFFICIENCY

◇ OUTPUT COUPLING EFF

✱ TOTAL EFFICIENCY

□ E-FIELD MAX

ASYMMETRIC MIRRORS

GX=.75

4% LOSSES

Figure 14d

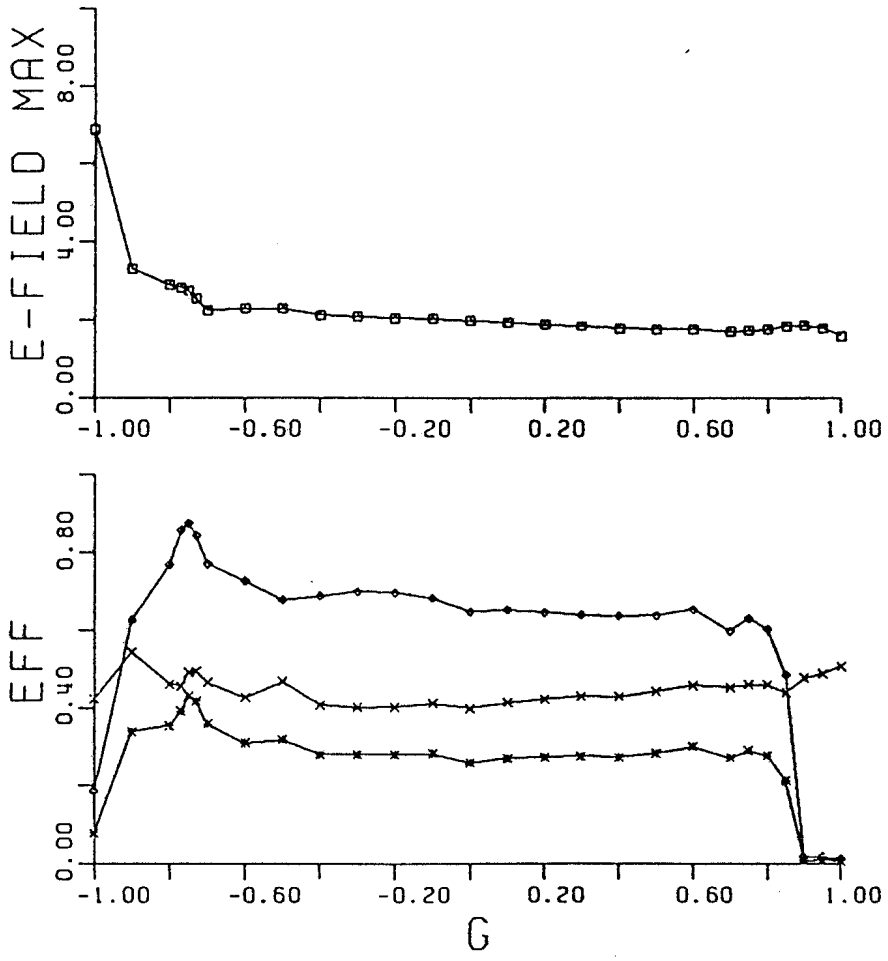

× ELECTRONIC EFFICIENCY

◇ OUTPUT COUPLING EFF

✱ TOTAL EFFICIENCY

□ E-FIELD MAX

ELLIPTICAL MIRRORS

GX=-.75

Figure 14e

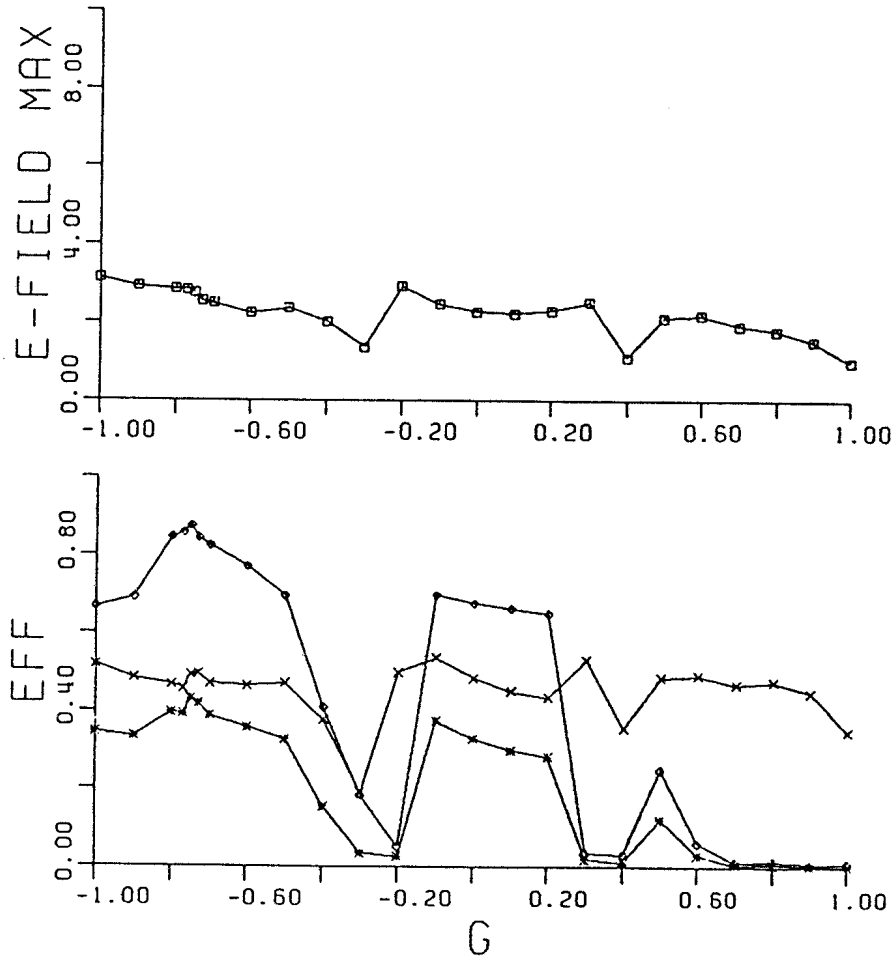

× ELECTRONIC EFFICIENCY

◇ OUTPUT COUPLING EFF

✱ TOTAL EFFICIENCY

□ E-FIELD MAX

ASYMETRIC MIRRORS

GX=-.75

4% LOSSES

Figure 14f

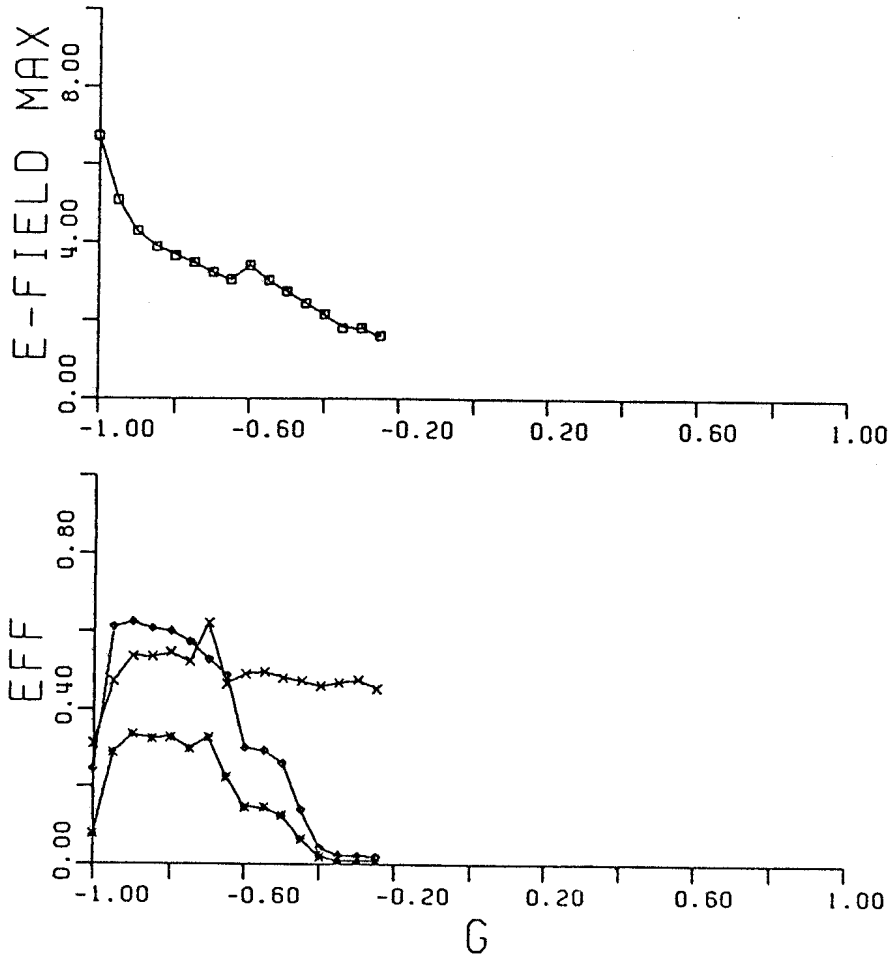

× ELECTRONIC EFFICIENCY

◇ OUTPUT COUPLING EFF

✱ TOTAL EFFICIENCY

□ E-FIELD MAX

ASYMETRIC MIRRORS

GX=.75

4% LOSSES

Figure 14g

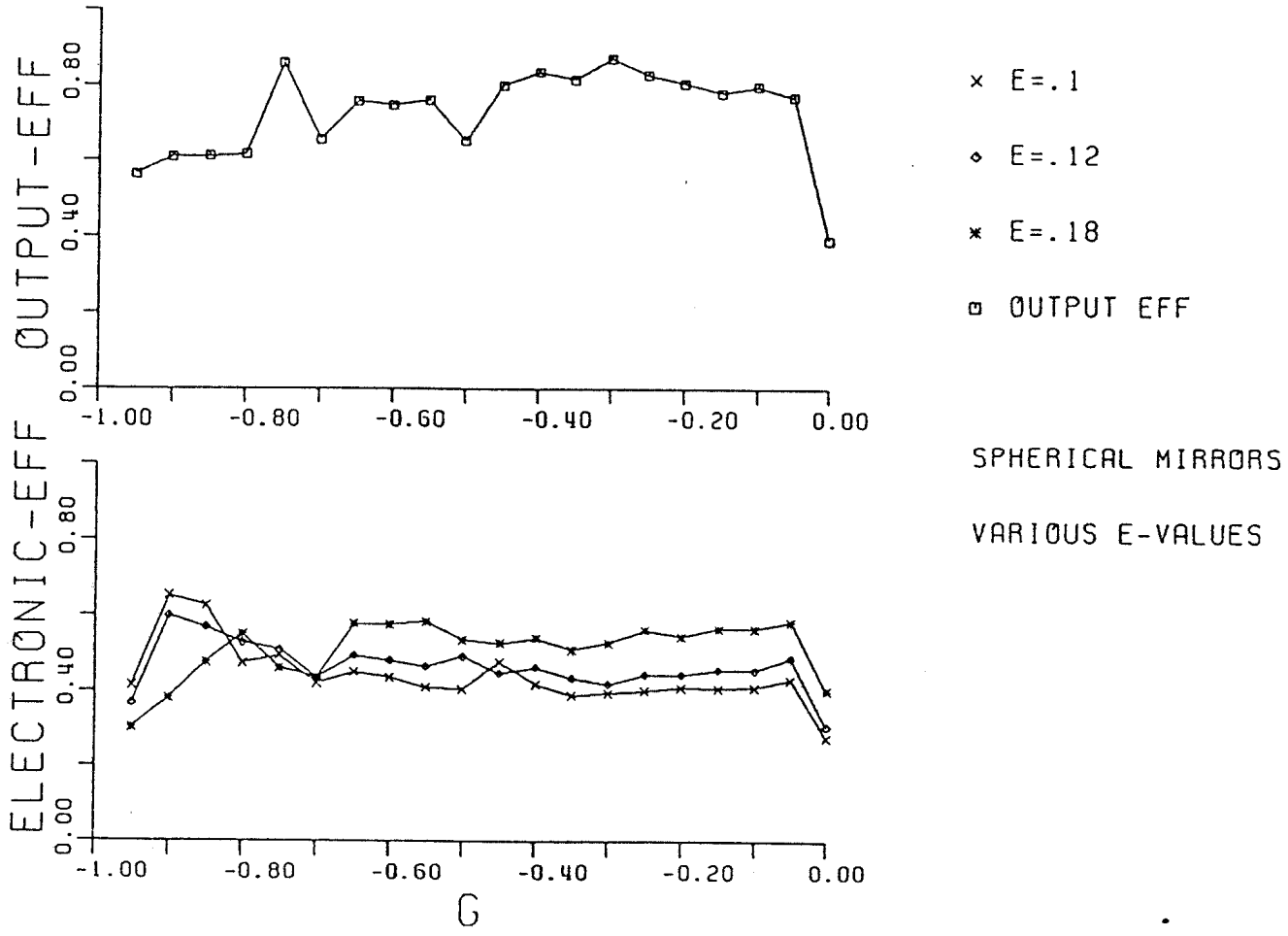
OUTPUT-EFF
0.80
0.40
0.00
-1.00
-0.80
-0.60
-0.40
-0.20
0.00
ELECTRONIC-EFF
0.80
0.40
0.00
-1.00
-0.80
-0.60
-0.40
-0.20
0.00
G
× E=.1
◇ E=.12
* E=.18
□ OUTPUT EFF
SPHERICAL MIRRORS
VARIOUS E-VALUES

Figure 15a

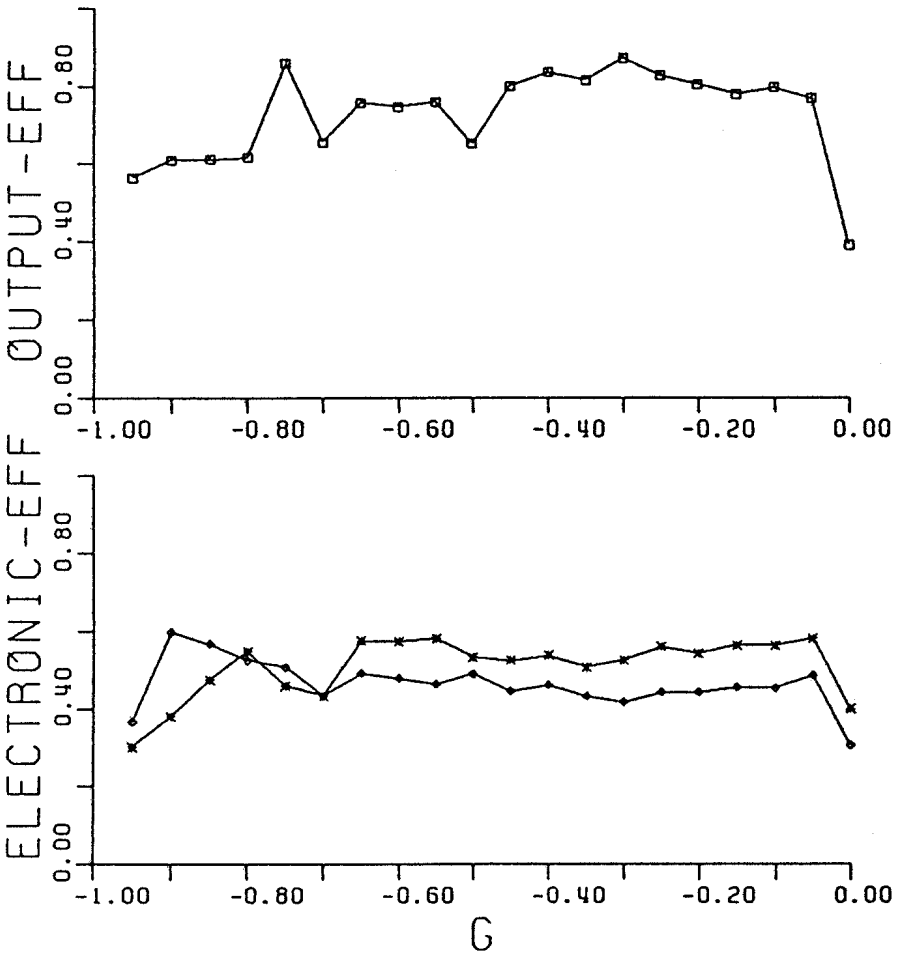
OUTPUT-EFF
0.00
0.40
0.80
-1.00
-0.80
-0.60
-0.40
-0.20
0.00
ELECTRONIC-EFF
0.00
0.40
0.80
-1.00
-0.80
-0.60
-0.40
-0.20
0.00
G
◇ E=.12 (BRASS)
✱ E=.18 (COPPER)
▫ OUTPUT EFF
SPHERICAL MIRRORS
MAXIMAL HEAT LOAD
=1.5KW/CM**2

Figure 15b

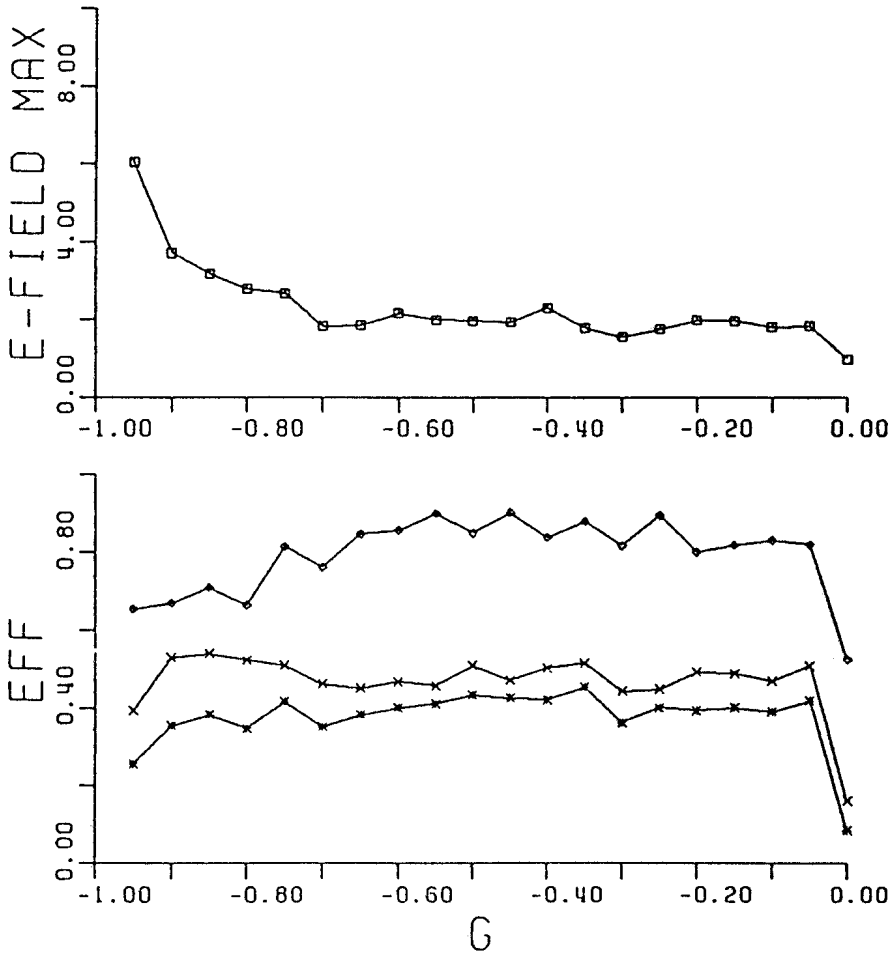

× ELECTRONIC EFFICIENCY

◇ OUTPUT COUPLING EFF

✱ TOTAL EFFICIENCY

□ E-FIELD MAX

SPHERICAL MIRRORS

10% LOSSES

E=.12

Figure 16a

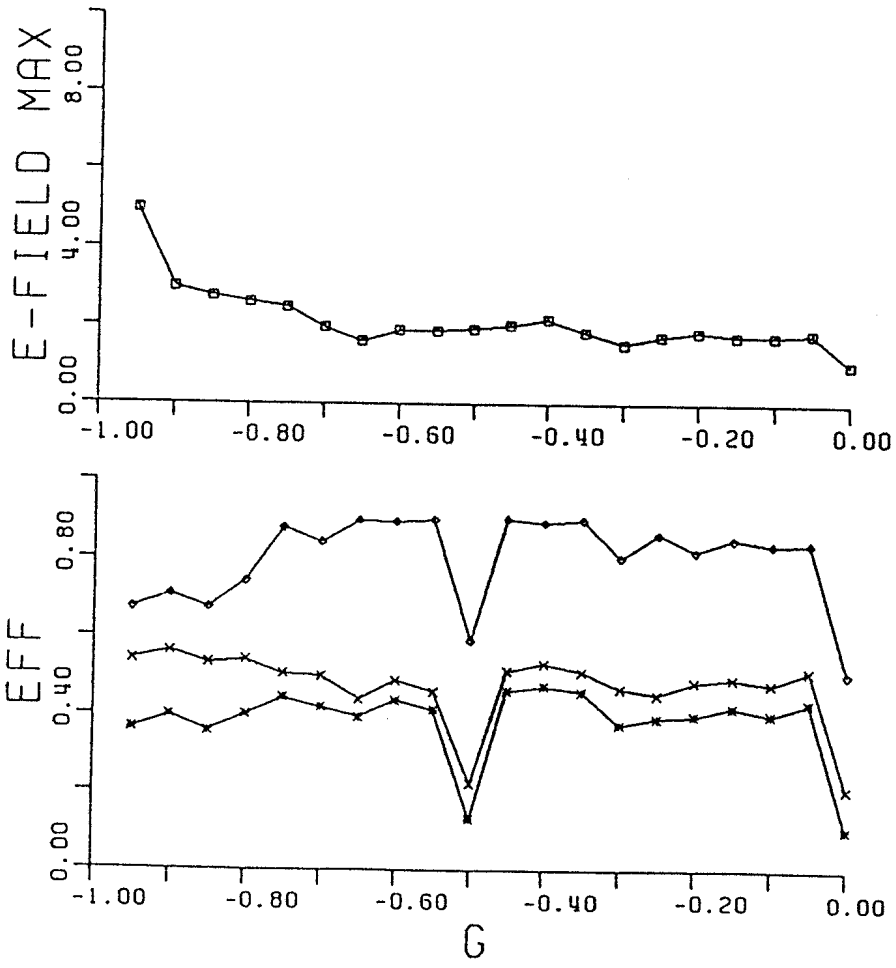

× ELECTRONIC EFFICIENCY

◇ OUTPUT COUPLING EFF

✱ TOTAL EFFICIENCY

□ E-FIELD MAX

SPHERICAL MIRRORS

20% LOSSES

E=.12

Figure 16b